



Splines Finite Element Solver for One-Dimensional Time-Dependent Maxwell’s Equations via Fourier Transform Discretization

Imad EL BARKANI and Mohamed ADDAM

ABSTRACT: In this article, we solve the time-dependent Maxwell coupled equations in their one-dimensional version relatively to space-variable. We effectuate a variable reduction via Fourier transform to make the time variable as a frequency parameter easy and quickly to manage. A Galerkin variational method based on higher-order spline interpolations is used to approximate the solution relatively to the spacial variable. So, the state of existence of the solution, its uniqueness, and its regularity are studied and proved, and the study is also provided by an error estimate and the convergence orders of the proposed method. Also, we use the critical Nyquist frequency to calculate numerically the solution of the Inverse Fourier Transform(IFT); and for all numerical computations, we consider several quadrature methods. Finally, we give some experiments to illustrate the success of such an approach.

Key Words: 1D Maxwell wave equation, Fourier Transform Discretization, Splines finite element approximation, quadrature methods, error estimates, signal reconstruction, Convergence Orders.

Contents

1 Introduction	1
2 Governing electromagnetic Maxwell’s equations	2
3 Overview on Normalized Uniform Polynomial Splines (NUPS)	3
4 Fourier Transform Approach Framework	4
4.1 1D wave problem in frequency-domain	4
4.2 A weak variational formulation	6
4.3 γ -Splines finite element approximation	9
5 Quadrature computations for time-dependent solutions	11
6 Convergence analysis and error estimate	13
7 Numerical results and order of convergence	18
7.1 Time-dependent Harmonic solution of 1D Maxwell’s equations	18
7.2 Accuracy test for one-dimensional Maxwell’s equations	19
7.3 Rastrigin solutions for one-dimensional Maxwell’s equations	21
7.4 Verification test for one-dimensional Maxwell’s equations	21
7.5 Convergence orders	23
8 Conclusions	24

1. Introduction

Maxwell’s wave state model, or electromagnetic wave propagation, relies on numerous technology areas. The elastic system models mechanical waves in solids and fluids, respectively. The acoustic wave equation and the Maxwell equations describe the propagation of electromagnetic waves. Current societies use electromagnetic wave propagation phenomena to solve significant problems: Medical Imaging devices [16], seismic wave engineering [8,27], mobile communications and transmission lines, geophysics for oil exploration [8,28], and electrical power generation [15]. Another aspect is to recover the electromagnetic

2010 *Mathematics Subject Classification:* 65D05, 65D07, 65D30, 65D32, 65E05, 65F30, 65G20, 65M60.

Submitted November 21, 2022. Published April 24, 2023

signal by solving the linear Maxwell's problems; thus, the electric signal and the induced magnetic signal are solutions of the above equations [6,7,12,30]. Multiple examples of technologies are strongly reliant on electromagnetic wave propagation [11,23]. Moreover, numerous deterministic partial differential equations (PDE) have governed such a domain since the 19th and 20th centuries. Modeling wave propagation for realistic engineering problems requires numerical computations based on approximation and interpolation methods. Several researchers and engineers continue developing computational methods to solve the PDE propagation of the electromagnetic wave (radio waves or light propagation). The electromagnetic wave problem is employed as a current model for describing moving waves technology propagation. So, the robust and accurate numerical approximation of the wave equations is essential and fundamental for simulation in different application areas. Several models for all kinds of waves, which have various degrees of complexity, are given in much scientific work. In the current literature, there exists much work attractive to the computational areas of wave propagation equations [11,14,19,21,22,23,27,28,29,30]; for example, the Helmholtz state equation, which governs the harmonic wave problems, is primarily treated.

The model studied in this work is a headmistress or primary source of several practical problems in electromagnetism, wave propagation, and signal transmission [24,26]. For example, it's used to manage the elements of the electromagnetic signal and represent the components as a careful and well-regulated solution for low vibration propagating over long distances. Our aim is to use and adapt the higher-order spline functions for signal decomposition over long amplitude domains. The higher-order γ of the spline functions allows a benefit at the level of signal reconstruction by using its components over large fields with a reduced computational cost.

We propose a higher-order spline interpolating method to find the time-dependent signal based on one-dimensional Maxwell's electromagnetic equations. Also, the reconstructed signal is the unique solution to the electromagnetic transport problem. As in [1,2], we employ the Fourier Transform Discretization(FTD), which implies an equivalent coupled Maxwell's equations dependent on the frequency parameter. Some numerical techniques are employed to solve the coupled Maxwell's electromagnetic wave problem. So, the equivalent equation depending on the frequency parameter is resolved using the γ -splines finite element method; here, the coefficient γ represents the order or degree of the spline functions. The quadrature methods are used to determine the computed signal like a solution calculated as the IFT of the obtained solution of a frequency variable; we also show the Gauss-Hermite quadrature, Rectangle's quadrature, Trapezoidal quadrature, Simpson's quadrature, and Gauss quadrature method. These quadrature techniques are used to compute the time-domain magnitude density as the IFT of the magnitude density in the frequency area concerning the time variable.

The paper is well-organized as follows: In Section 2, we give a brief overview of the deterministic Maxwell's wave equations equipped by the Dirichlet boundary conditions. Section 3 illustrates a short review of Normalized Uniform Polynomial Splines (NUPS) used as a spatial approximation tool or technique. In section 4, we employ the FTD in which we show the state of existence, uniqueness, and smoothness of Maxwell's wave transport equations in frequency media approach; after this, an approximation of the magnitude density and the electrical density for the frequency variable is also expressed by using a γ -spline function Galerkin projection interpolated method. In section 5, we used several quadrature formulations to compute the IFT of the temporal magnitude signal with respect to the time variable and ended with an optimal algorithm that expands all the steps of our study. Convergence and error estimates are reviewed in Section 6. Finally, a few numerical examples illustrating the signal reconstruction in the homogenous and heterogeneous media, analysis, and convergence orders are presented in Section 7, which concluded with a few relevant remarks and an outlook for prospective work.

2. Governing electromagnetic Maxwell's equations

We consider Maxwell's equations or wave problem to be his one-dimensional version. Let t_o and T represent the initial and period times, respectively. Let $[a, b] \subset \mathbb{R}$ and $[t_o, t_o + T]$ be the space and time domains, respectively. We denote by $\phi(x, t)$ the electric density and $\psi(x, t)$ the magnitude density. The functions ϕ and ψ depend on the space variables $x \in]a, b[$ and the time variable $t \in [t_o, t_o + T]$. The magnetic permeability μ and the electrical permittivity ε are positive bounded functions given by $\mu(x) = \mu_0 \mu_r(x)$ and $\varepsilon(x) = \varepsilon_0 \varepsilon_r(x) \quad \forall x \in [a, b]$, where μ_r is the magnetic permeability and ε_r is the electrical permittivity of the work domain, and μ_0 is the magnetic permeability and ε_0 is the electrical

permittivity of the vacuum. We recall that the speed of light in the vacuum is given by $c_o = 1/\sqrt{\mu_0 \varepsilon_0}$ and the speed of light through the considered domain is given by $c(x) = 1/\sqrt{\mu(x) \varepsilon(x)}$. We consider the time-dependent electromagnetic wave problem for the magnitude density and the electric density reconstruction. The pair densities $(\phi(x, t), \psi(x, t))$ yield the hyperbolic deterministic electromagnetic wave problem, also known as the 1D-Maxwell's problem, and satisfy the coupled equations shown below:

$$\begin{cases} \varepsilon(x) \frac{\partial \phi(x, t)}{\partial t} + \frac{\partial \psi(x, t)}{\partial x} = f(x, t), \\ \mu(x) \frac{\partial \psi(x, t)}{\partial t} + \frac{\partial \phi(x, t)}{\partial x} = g(x, t) \end{cases} \quad (2.1)$$

for all $(x, t) \in]a, b[\times]t_o, t_o + T]$, with the initial conditions

$$\phi(x, t_o) = \phi_0(x) \quad \text{and} \quad \psi(x, t_o) = \psi_0(x) \quad \text{for all } x \in [a, b], \quad (2.2)$$

where ϕ_0 and ψ_0 are given initial functions. As usual, the functions $f(x, t)$ and $g(x, t)$ prescribe the internal source terms. The previous derivatives are utilized in a distribution or weak derivatives sense. Hence, the considered boundary conditions for the transverse electromagnetic equation (2.1) are

$$\begin{cases} \phi(a, t) = -g_a(t), & \phi(b, t) = g_b(t) \\ \psi(a, t) = -h_a(t), & \psi(b, t) = h_b(t) \end{cases} \quad (2.3)$$

for all $t \in [t_o, t_o + T]$ and g_a, g_b, h_a and h_b prescribes the boundary functions. In this article, we will suppose that the real-valued coefficients μ and ε are a positive bounded functions belonging to $L^\infty(a, b)$. Furthermore, the system (2.1)-(2.2)-(2.3) described the boundary-value problem studied in this study.

3. Overview on Normalized Uniform Polynomial Splines (NUPS)

As in [1,9,18], the elementary basis functions $\mathbf{N}_{i,\gamma}$ are obtained by the following scheme

$$\begin{cases} \mathbf{N}_{i,0}(\zeta) = 1, & \text{if } i \leq \zeta \leq i+1, \quad \text{and} \quad \mathbf{N}_{i,0}(\zeta) = 0, \quad \text{otherwise,} \\ \mathbf{N}_{i,\gamma}(\zeta) = \lambda_{i,\gamma}(\zeta) \mathbf{N}_{i-1,\gamma-1}(\zeta) + (1 - \lambda_{i+1,\gamma}(\zeta)) \mathbf{N}_{i,\gamma-1}(\zeta), \end{cases} \quad (3.1)$$

for $i = 1, \dots, \gamma - 1$, where $\lambda_{i,\gamma}(\zeta) = \frac{\gamma-i+\zeta}{\gamma}$ for all $\gamma \geq 1$ and $\zeta \in [0, 1]$.

For $\gamma \geq 0$, the basis functions $\mathbf{N}_{i,\gamma}$ are illustrated in the scheme (3.1). then for $0 \leq i \leq 6$ and $0 \leq \gamma \leq 6$, the elementary basis functions $\mathbf{N}_{i,\gamma}$ are given by

$$\begin{aligned} \mathbf{N}_{0,1}(\zeta) &= 1 - \zeta, \quad \mathbf{N}_{1,1}(\zeta) = \zeta, \quad \mathbf{N}_{0,2}(\zeta) = \frac{1}{2}(1 - \zeta)^2, \quad \mathbf{N}_{1,2}(\zeta) = \frac{1}{2}(1 + 2\zeta - 2\zeta^2), \quad \mathbf{N}_{2,2}(\zeta) = \frac{1}{2}\zeta^2, \\ \mathbf{N}_{0,3}(\zeta) &= \frac{1}{6}(1 - \zeta)^3, \quad \mathbf{N}_{1,3}(\zeta) = \frac{1}{6}(4 - 6\zeta^2 + 3\zeta^3), \quad \mathbf{N}_{2,3}(\zeta) = \frac{1}{6}(1 + 3\zeta + 3\zeta^2 - 3\zeta^3), \quad \mathbf{N}_{3,3}(\zeta) = \frac{1}{6}\zeta^3, \\ \mathbf{N}_{0,4}(\zeta) &= \frac{1}{24}(1 - \zeta)^4, \quad \mathbf{N}_{1,4}(\zeta) = \frac{1}{24}(11 - 12\zeta - 6\zeta^2 + 12\zeta^3 - 4\zeta^4), \quad \mathbf{N}_{2,4}(\zeta) = \frac{1}{24}(11 + 12\zeta - 6\zeta^2 - 12\zeta^3 + 6\zeta^4), \\ \mathbf{N}_{3,4}(\zeta) &= \frac{1}{24}(1 + 4\zeta + 6\zeta^2 + 4\zeta^3 - 4\zeta^4), \quad \mathbf{N}_{4,4}(\zeta) = \frac{1}{24}\zeta^4. \\ \mathbf{N}_{0,5}(\zeta) &= \frac{1}{120}(1 - \zeta)^5, \quad \mathbf{N}_{1,5}(\zeta) = \frac{1}{120}(26 - 50\zeta + 20\zeta^2 + 20\zeta^3 - 20\zeta^4 + 5\zeta^5), \quad \mathbf{N}_{2,5}(\zeta) = \frac{1}{120}(66 - 60\zeta^2 + 30\zeta^4 - 10\zeta^5), \\ \mathbf{N}_{3,5}(\zeta) &= \frac{1}{120}(26 + 50\zeta + 20\zeta^2 - 20\zeta^3 - 20\zeta^4 + 10\zeta^5), \quad \mathbf{N}_{4,5}(\zeta) = \frac{1}{120}(1 + 5\zeta + 10\zeta^2 + 10\zeta^3 + 5\zeta^4 - 5\zeta^5), \\ \mathbf{N}_{5,5}(\zeta) &= \frac{1}{120}\zeta^5, \\ \mathbf{N}_{0,6}(\zeta) &= \frac{1}{720}(1 - \zeta)^6, \quad \mathbf{N}_{1,6}(\zeta) = \frac{1}{720}(57 - 150\zeta + 135\zeta^2 - 20\zeta^3 - 45\zeta^4 + 30\zeta^5 - 6\zeta^6), \quad \mathbf{N}_{2,6}(\zeta) = \frac{1}{720}(302 - 240\zeta - \\ &150\zeta^2 + 160\zeta^3 + 30\zeta^4 - 60\zeta^5 + 15\zeta^6), \quad \mathbf{N}_{3,6}(\zeta) = \frac{1}{720}(302 + 240\zeta - 150\zeta^2 - 160\zeta^3 + 30\zeta^4 + 60\zeta^5 - 20\zeta^6), \quad \mathbf{N}_{4,6}(\zeta) = \\ &\frac{1}{720}(57 + 150\zeta + 135\zeta^2 + 20\zeta^3 - 45\zeta^4 - 30\zeta^5 + 15\zeta^6), \quad \mathbf{N}_{5,6}(\zeta) = \frac{1}{720}(1 + 6\zeta + 15\zeta^2 + 20\zeta^3 + 15\zeta^4 + 6\zeta^5 - 6\zeta^6), \\ \mathbf{N}_{6,6}(\zeta) &= \frac{1}{720}\zeta^6. \end{aligned}$$

It's easy to see that the reference basis of splines $\mathbf{N}_{i,\gamma}$ for $\gamma \in \mathbb{N}$ is normalized in the following sense :

$$\sum_{i \in \mathbb{Z}} \mathbf{N}_{i,\gamma}(\zeta) = 1, \quad \text{for all } \zeta \in [0, 1]. \quad (3.2)$$

As a result, the classical normalized uniform polynomial spline \mathbf{B}_γ of degree $\gamma \in \mathbb{N}$ with support embedding in $[0, \gamma + 1]$ is defined by

$$\mathbf{B}_\gamma(\xi) = \begin{cases} \mathbf{N}_{\gamma-i,\gamma}(\xi - i), & \text{for } i \leq \xi \leq i+1, \quad i = 0, \dots, \gamma, \\ 0, & \text{for } \xi \leq 0, \quad \gamma + 1 \leq \xi. \end{cases} \quad (3.3)$$

Also, the normalized uniform spline \mathbf{B}_γ is a piecewise polynomial function of degree γ with integer knot points and is $\mathcal{C}^{\gamma-1}$ -class functions.

The normalized uniform splines functions $(\mathbf{B}_\gamma)_{0 \leq \gamma \leq 6}$ are computed by using the relationship Eq.(3.3), also we obtain

$$\begin{aligned}
\mathbf{B}_0 &= \mathbb{1}_{[0,1[}, & \mathbf{B}_1 &= \xi \mathbb{1}_{[0,1[} + (2 - \xi) \mathbb{1}_{[1,2[}, \\
\mathbf{B}_2 &= \frac{1}{2}\xi^2 \mathbb{1}_{[0,1[} + \frac{1}{2}(-3 + 6\xi - 2\xi^2) \mathbb{1}_{[1,2[} + \frac{1}{2}(\xi - 3)^2 \mathbb{1}_{[2,3[} \\
\mathbf{B}_3 &= \frac{1}{6}\xi^3 \mathbb{1}_{[0,1[} + \frac{1}{6}(-3\xi^3 + 12\xi^2 - 12\xi + 4) \mathbb{1}_{[1,2[} \\
&\quad + \frac{1}{6}(3\xi^3 - 24\xi^2 + 60\xi - 44) \mathbb{1}_{[2,3[} + \frac{1}{6}(4 - \xi)^3 \mathbb{1}_{[3,4[} \\
\mathbf{B}_4 &= \frac{1}{24}\xi^4 \mathbb{1}_{[0,1[} + \frac{1}{24}(-4\xi^4 + 20\xi^3 - 30\xi^2 + 20\xi - 5) \mathbb{1}_{[1,2[} \\
&\quad + \frac{1}{24}(6\xi^4 - 60\xi^3 + 210\xi^2 - 300\xi + 155) \mathbb{1}_{[2,3[} \\
&\quad + \frac{1}{24}(-4\xi^4 + 60\xi^3 - 330\xi^2 + 780\xi - 655) \mathbb{1}_{[3,4[} + \frac{1}{24}(\xi - 5)^4 \mathbb{1}_{[4,5[}, \\
\mathbf{B}_5 &= \frac{1}{120}\xi^5 \mathbb{1}_{[0,1[} + \frac{1}{120}(6 - 30\xi + 60\xi^2 - 60\xi^3 + 30\xi^4 - 5\xi^5) \mathbb{1}_{[1,2[} \\
&\quad + \frac{1}{120}(10\xi^5 - 120\xi^4 + 540\xi^3 - 1140\xi^2 + 1170\xi - 474) \mathbb{1}_{[2,3[} \\
&\quad + \frac{1}{120}(-10\xi^5 + 180\xi^4 - 1260\xi^3 + 4260\xi^2 - 6930\xi + 4) \mathbb{1}_{[3,4[} \\
&\quad + \frac{1}{120}(5\xi^5 - 120\xi^4 + 1140\xi^3 - 5340\xi^2 + 12270\xi - 10974) \mathbb{1}_{[4,5[} \\
&\quad + \frac{1}{120}(6 - \xi)^5 \mathbb{1}_{[5,6[} \\
\mathbf{B}_6 &= \frac{1}{720}\xi^6 \mathbb{1}_{[0,1[} + \frac{1}{720}(-7 + 42\xi - 105\xi^2 + 140\xi^3 - 105\xi^4 + 42\xi^5 - 6\xi^6) \mathbb{1}_{[1,2[} \\
&\quad + \frac{1}{720}(1337 - 3990\xi + 4935\xi^2 - 3220\xi^3 + 1155\xi^4 - 210\xi^5 + 15\xi^6) \mathbb{1}_{[2,3[} \\
&\quad + \frac{1}{720}(-24178 + 47040\xi - 37590\xi^2 + 15680\xi^3 - 3570\xi^4 + 420\xi^5 - 20\xi^6) \mathbb{1}_{[3,4[} \\
&\quad + \frac{1}{720}(119182 - 168000\xi + 96810\xi^2 - 29120\xi^3 + 4830\xi^4 - 420\xi^5 + 15\xi^6) \mathbb{1}_{[4,5[} \\
&\quad + \frac{1}{720}(-208943 + 225750\xi - 100065\xi^2 + 23380\xi^3 - 3045\xi^4 + 210\xi^5 - 6\xi^6) \mathbb{1}_{[5,6[} \\
&\quad + \frac{1}{720}(7 - \xi)^6 \mathbb{1}_{[6,7]},
\end{aligned}$$

where $\mathbb{1}_{\mathbf{I}}$ is the characteristic function of the interval \mathbf{I} .

Furthermore, the spline \mathbf{B}_γ of degree $\gamma \in \mathbb{N}$, satisfied the following normalized criterium :

$$\int_{-\infty}^{+\infty} \mathbf{B}_\gamma(\xi) d\xi = \int_0^{\gamma+1} \mathbf{B}_\gamma(\xi) d\xi = 1, \quad \text{for all } \gamma \in \mathbb{N}. \quad (3.4)$$

Figure 2 depicts the plots of the normalized uniform spline functions $(\mathbf{B}_\gamma)_{0 \leq \gamma \leq 10}$.

4. Fourier Transform Approach Framework

4.1. 1D wave problem in frequency-domain

As in [1,2], we denote by $\widehat{L}_2 := L^2((a, b), \mathbb{C})$ the space of square integrable complex-valued functions on the domain $[a, b]$; and the space \widehat{L}_2 is endowed by its topology defined by the following inner product

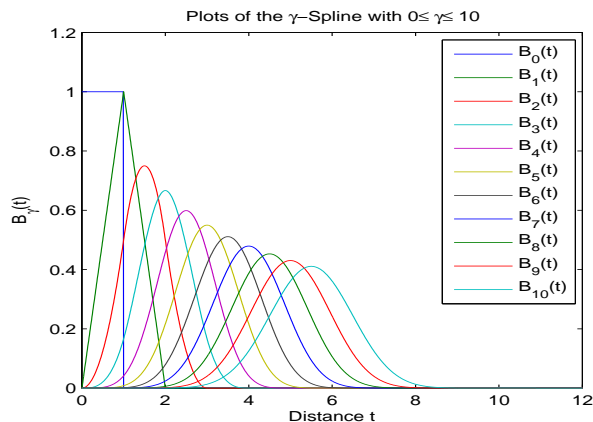


Figure 1: The plots of all γ -spline \mathbf{B}_γ on its supports $[0, \gamma + 1]$ for $0 \leq \gamma \leq 10$.

and its associated norm

$$(u|v)_2 = \int_a^b u(x)\overline{v(x)}dx, \quad \|u\|_2 = \sqrt{(u|u)_2}, \quad \forall u, v \in \widehat{L}_2.$$

In addition, for each $k \in \mathbb{N}$, we denote $\widehat{\mathbf{H}}_k = \mathbf{H}^k((a, b), \mathbb{C}) := \mathbf{W}^{k,2}((a, b), \mathbb{C})$ the Sobolev space endowed by its norm $\|\cdot\|_{\widehat{\mathbf{H}}_k}$ given by

$$\|u\|_{\widehat{\mathbf{H}}_k} = \left(\sum_{0 \leq \ell \leq k} \left\| \frac{\partial^\ell u}{\partial x^\ell} \right\|_2^2 \right)^{\frac{1}{2}}, \quad \forall u \in \widehat{\mathbf{H}}_k \quad (4.1)$$

where $\frac{\partial^\ell u}{\partial x^\ell}$ denote the distribution derivatives of u of order ℓ .

The classical space $L^2(]a, b[, \mathbb{R})$ of square integrable real-valued functions on the open interval $]a, b[$ is denoted by $L_2 := L^2(]a, b[, \mathbb{R})$ and \mathbf{H}_k denote the usual Sobolev space $\mathbf{H}_k = \mathbf{H}^k(]a, b[, \mathbb{R}) := \mathbf{W}^{k,2}(]a, b[, \mathbb{R})$ of real-valued functions. The space \mathbf{H}_k is equipped with the classical norm $\|\cdot\|_{\mathbf{H}_k}$ given as in (4.1).

For $1 \leq p < \infty$, the spaces $L^p(\mathbb{R}; \widehat{\mathbf{H}}_k)$ and $L^p(\mathbb{R}; \mathbf{H}_k)$ endowed with the norms

$$\begin{aligned} \|u\|_{L^p(\mathbb{R}; \widehat{\mathbf{H}}_k)} &= \left(\int_{-\infty}^{+\infty} \|u(\cdot, w)\|_{\widehat{\mathbf{H}}_k}^p dw \right)^{\frac{1}{p}}, \\ \|\phi\|_{L^p(\mathbb{R}; \mathbf{H}_k)} &= \left(\int_{-\infty}^{+\infty} \|\phi(\cdot, t)\|_{\mathbf{H}_k}^p dt \right)^{\frac{1}{p}}, \end{aligned} \quad (4.2)$$

respectively, are Banach spaces.

We assume that the function $t \mapsto \phi(x, t)$ and the derivative function $t \mapsto \frac{\partial \phi}{\partial x}(x, t)$ have extensions to \mathbb{R} belonging to the space $L^1(\mathbb{R}, \mathbb{R})$, almost everywhere in $[a, b]$. We also assume that the given source terms f, g, g_a, g_b, h_a and h_b have prolongations such that $f, g \in L^\infty(]a, b[; L^1(\mathbb{R}, \mathbb{R}))$ and $g_a, g_b, h_a, h_b \in L^1(\mathbb{R}, \mathbb{R})$. The Fourier transform \widehat{g} of a function g in $L^1(\mathbb{R}, \mathbb{R})$ is given by

$$\widehat{g}(w) = \frac{1}{\sqrt{2\pi}} \int_{-\infty}^{+\infty} g(t)e^{-iwt} dt, \quad i = \sqrt{-1}. \quad (4.3)$$

For succinct arguments based on the Lebesgue theorem of derivation under the integral sign, we also have

$$\widehat{\frac{\partial \phi}{\partial x}}(x, w) = \frac{\partial \widehat{\phi}}{\partial x}(x, w) \quad \text{and} \quad \widehat{\frac{\partial \psi}{\partial x}}(x, w) = \frac{\partial \widehat{\psi}}{\partial x}(x, w), \quad \forall (x, w) \in [a, b] \times \mathbb{R}. \quad (4.4)$$

We apply the Fourier transform to equation (2.1) together with the boundary conditions (2.3) and, we use the relationship $\frac{\partial \widehat{g}}{\partial t} = i\omega \widehat{g}$ and (4.4) to obtain the following Maxwell's wave equations satisfied by the wave functions in the frequency-domain

$$\begin{cases} i w \varepsilon(x) u(x, w) + \frac{\partial v}{\partial x}(x, w) = F(x, w), \\ i w \mu(x) v(x, w) + \frac{\partial u}{\partial x}(x, w) = G(x, w) \end{cases} \quad \forall (x, w) \in]a, b[\times \mathbb{R}, \quad (4.5)$$

with the following boundary conditions

$$\begin{cases} u(a, w) = -G_a(w), & u(b, w) = G_b(w) \\ v(a, w) = -H_a(w), & v(b, w) = H_b(w) \end{cases} \quad \text{for all } w \in \mathbb{R}, \quad (4.6)$$

where $u(\cdot, w) = \widehat{\phi}(\cdot, w)$, $v(\cdot, w) = \widehat{\psi}(\cdot, w)$, $F(\cdot, w) = \widehat{f}(\cdot, w)$, $G(\cdot, w) = \widehat{g}(\cdot, w)$, $G_a(w) = \widehat{g}_a(w)$, $G_b(w) = \widehat{g}_b(w)$, $H_a(w) = \widehat{h}_a(w)$, $H_b(w) = \widehat{h}_b(w)$ are the Fourier transforms with respect to the time variable t of $\phi(x, \cdot)$, $\psi(x, \cdot)$, $f(x, \cdot)$ and $g(x, \cdot)$, g_a , g_b , h_a and h_b , respectively.

4.2. A weak variational formulation

Let $U_*(\cdot, w) = (u_*(\cdot, w), v_*(\cdot, w))$ be a sufficiently smooth function satisfying the problem (4.5) and (4.6), such that $(u_*(\cdot, w), v_*(\cdot, w)) \in \widehat{H}_1 \times \widehat{H}_1$. By multiplying the coupled wave equation (4.5) by any of the pairs of test functions $(\overline{\varphi}, \overline{\theta}) \in \widehat{H}_1 \times \widehat{H}_1$ and integrating by parts over $[a, b]$ with respect to the boundary conditions (4.6), the following pairs of weak variational formulations equivalent to the Maxwell's electromagnetic wave problem in the frequency-domain are obtained:

$$\begin{cases} \mathcal{A}_w(u_*(\cdot, w), \varphi) + \mathcal{C}(v_*(\cdot, w), \varphi) = \mathcal{J}_w(\varphi), \\ \mathcal{B}_w(v_*(\cdot, w), \theta) + \mathcal{C}(u_*(\cdot, w), \theta) = \mathcal{K}_w(\theta), \end{cases} \quad (4.7)$$

where the sesquilinear forms $\mathcal{A}_w : \widehat{H}_1 \times \widehat{H}_1 \rightarrow \mathbb{C}$, $\mathcal{B}_w : \widehat{H}_1 \times \widehat{H}_1 \rightarrow \mathbb{C}$ and $\mathcal{C} : \widehat{H}_1 \times \widehat{H}_1 \rightarrow \mathbb{C}$, are defined for all u, v, φ and θ in \widehat{H}_1 by

$$\begin{aligned} \mathcal{A}_w(u, \varphi) &= i w \int_a^b \varepsilon(x) u(x) \overline{\varphi(x)} dx, & \mathcal{B}_w(v, \theta) &= i w \int_a^b \mu(x) v(x) \overline{\theta(x)} dx, \\ \mathcal{C}(v, \varphi) &= - \int_a^b v(x) \frac{\partial \overline{\varphi(x)}}{\partial x} dx & \text{and} & \quad \mathcal{C}(u, \theta) = - \int_a^b u(x) \frac{\partial \overline{\theta(x)}}{\partial x} dx \end{aligned} \quad (4.8)$$

respectively, and the semi-linear forms $\mathcal{J}_w : \widehat{H}_1 \rightarrow \mathbb{C}$ and $\mathcal{K}_w : \widehat{H}_1 \rightarrow \mathbb{C}$, re defined for all φ and θ in \widehat{H}_1 by

$$\begin{aligned} \mathcal{J}_w(\varphi) &= \int_a^b F(x, w) \overline{\varphi(x)} dx - H_b(w) \overline{\varphi(b)} - H_a(w) \overline{\varphi(a)}, \\ \mathcal{K}_w(\theta) &= \int_a^b G(x, w) \overline{\theta(x)} dx - G_b(w) \overline{\theta(b)} - G_a(w) \overline{\theta(a)}, \end{aligned} \quad (4.9)$$

respectively. Add the sesquilinear forms \mathcal{A}_w , \mathcal{B}_w and \mathcal{C} on one hand, and the semi-linear forms \mathcal{J}_w and \mathcal{K}_w , we get the equivalent weak variational formulation:

$$\mathcal{A}_w(U_*(\cdot, w), V) = \mathcal{L}_w(V), \quad \forall V \in \widehat{E} := \widehat{H}_1 \times \widehat{H}_1 \quad (4.10)$$

where $V = (\varphi, \theta)$, and the sesquilinear form $\mathcal{A}_w : \widehat{E} \times \widehat{E} \rightarrow \mathbb{C}$ and the semi-linear form $\mathcal{L}_w : \widehat{E} \rightarrow \mathbb{C}$ are defined for all $U = (u, v)$ and $V = (\varphi, \theta)$ in \widehat{E} by

$$\mathcal{A}_w(U, V) = \mathcal{A}_w(u, \varphi) + \mathcal{B}_w(v, \theta) + \mathcal{C}(v, \varphi) + \mathcal{C}(u, \theta) \quad \text{and} \quad \mathcal{L}_w(V) = \mathcal{J}_w(\varphi) + \mathcal{K}_w(\theta)$$

for all $(\varphi, \theta) \in \widehat{\mathbb{E}}$, respectively. Conversely, let $U_*(\cdot, w) = (u_*(\cdot, w), v_*(\cdot, w))$ satisfying the weak variational formulation (4.10). An integration by parts demonstrates that

$$\begin{aligned} & \int_a^b \left(i w \varepsilon(x) u_*(x, w) + \frac{\partial v_*}{\partial x}(x, w) - F(x, w) \right) \overline{\varphi(x)} dx \\ & + \int_a^b \left(i w \mu(x) v_*(x, w) + \frac{\partial u_*}{\partial x}(x, w) - G(x, w) \right) \overline{\theta(x)} dx \\ & = (G_a(w) + u_*(a, w)) \overline{\varphi(a)} + (G_b(w) - u_*(b, w)) \overline{\varphi(b)} + \\ & (H_a(w) + v_*(a, w)) \overline{\theta(a)} + (H_b(w) - v_*(b, w)) \overline{\theta(b)}, \end{aligned} \quad (4.11)$$

for all $V = (\varphi, \theta)$ in $\widehat{\mathbb{E}}$. In particular, for a C^∞ of pair of functions $V = (\chi, 0)$ where χ is a compact support $\subset]a, b[$, we get

$$\int_a^b \left(i w \varepsilon(x) u_*(x, w) + \frac{\partial v_*}{\partial x}(x, w) - F(x, w) \right) \overline{\chi(x)}(x) dx = 0$$

on the one hand, and on the other hand, for a pair of C^∞ functions $V = (0, \vartheta)$ where ϑ is a compact support $\subset]a, b[$, we get

$$\int_a^b \left(i w \mu(x) v_*(x, w) + \frac{\partial u_*}{\partial x}(x, w) - G(x, w) \right) \overline{\vartheta(x)}(x) dx = 0.$$

Thus, in the distribution sense, we have

$$\begin{cases} i w \varepsilon(\cdot) u_*(\cdot, w) + \frac{\partial v_*}{\partial x}(\cdot, w) = F(\cdot, w), \\ i w \mu(\cdot) v_*(\cdot, w) + \frac{\partial u_*}{\partial x}(\cdot, w) = G(\cdot, w) \end{cases} \quad \text{on }]a, b[. \quad (4.12)$$

Since the functions f and g are assumed to be in $L^\infty(]a, b[; L^1(\mathbb{R}, \mathbb{R}))$, it follows that $F(\cdot, w)$ and $G(\cdot, w)$ belongs to the space $L^\infty(]a, b[, \mathbb{C})$. Thus, the previous equality holds almost everywhere in $]a, b[$.

Now, let $(\chi_1, 0)$ and $(\chi_2, 0)$ be two pairs of functions in $\widehat{\mathbb{H}}_1 \times \widehat{\mathbb{H}}_1$ such that $\chi_1(a) = \chi_2(b) = 1$ and $\chi_1(b) = \chi_2(a) = 0$. By setting $\varphi = \chi_1$ and $\varphi = \chi_2$, in (4.11), we get $G_a(w) = -u_*(a, w)$ and $G_b(w) = u_*(b, w)$ respectively, and let $(0, \vartheta_1)$ and $(0, \vartheta_2)$ be two pairs of functions in $\widehat{\mathbb{H}}_1 \times \widehat{\mathbb{H}}_1$ such that $\vartheta_1(a) = \vartheta_2(b) = 1$ and $\vartheta_1(b) = \vartheta_2(a) = 0$. By setting $\theta = \vartheta_1$ and $\theta = \vartheta_2$, in (4.11), we get $H_a(w) = -v_*(a, w)$ and $H_b(w) = v_*(a, w)$ respectively. In conclusion, the problem (4.5)-(4.6) is equivalent to the weak variational formulation (4.10).

According to the Sobolev continuous embedding theorem, there exists a constant $c_1 > 0$ that depends only on a and b , such that

$$\sup_{x \in [a, b]} \{|u(x)|, |v(x)|\} \leq c_1 \|U\|_{\widehat{L}_2 \times \widehat{L}_2}, \quad \forall U = (u, v) \in \widehat{\mathbb{E}}. \quad (4.13)$$

Using the Schwarz inequality and the Sobolev continuous embedding theorem, it follows that there exists a constant $c_2 > 0$ that depends only on a and b , such that

$$|\mathcal{L}_w(V)| \leq M(w) \|V\|_{\widehat{L}_2 \times \widehat{L}_2}, \quad \forall V \in \widehat{\mathbb{E}}, \quad (4.14)$$

where $M(w) = c_2(\|F(\cdot, w)\|_{\widehat{L}_2} + \|G(\cdot, w)\|_{\widehat{L}_2} + |G_a(w)|_{\mathbb{C}} + |G_b(w)|_{\mathbb{C}} + |H_a(w)|_{\mathbb{C}} + |H_b(w)|_{\mathbb{C}})$. Therefore, the operator $\mathcal{L}_w : \widehat{\mathbb{H}}_1 \times \widehat{\mathbb{H}}_1 \rightarrow \mathbb{C}$ is a continuous semi-linear form on $\widehat{\mathbb{H}}_1 \times \widehat{\mathbb{H}}_1$. Using the Sobolev continuous embedding theorem, there exists a nonnegative constant $c_3 > 0$ that is independent of the frequency w , such that

$$|\mathcal{A}_w(U, V)| \leq c_3(1 + w^2)^{\frac{1}{2}} \|U\|_{\widehat{L}_2 \times \widehat{L}_2} \|V\|_{\widehat{L}_2 \times \widehat{L}_2}, \quad \forall U, V \in \widehat{\mathbb{H}}_1 \times \widehat{\mathbb{H}}_1. \quad (4.15)$$

Hence, the coercivity or ellipticity of the sesquilinear form \mathcal{A}_w given in (4.10) is also proved by the following Lemma,

Lemma 4.1. *Let w be a real fixed frequency, the sesquilinear form \mathcal{A}_w given in Eq.(4.10) is elliptic on a subspace $\mathcal{H} \subseteq \widehat{\mathbf{H}}_1 \times \widehat{\mathbf{H}}_1 := \widehat{\mathbf{E}}$.*

Furthermore, for every $U \in \mathcal{H} \subseteq \widehat{\mathbf{H}}_1 \times \widehat{\mathbf{H}}_1$ we have

$$|\mathcal{A}_w(U, U)| \geq \alpha \|U\|_{\widehat{\mathbf{L}}_2 \times \widehat{\mathbf{L}}_2}^2. \quad (4.16)$$

Proof. For every $U = (u, v) \in \widehat{\mathbf{H}}_1 \times \widehat{\mathbf{H}}_1$ we have

$$\mathcal{A}_w(U, U) = i w \int_a^b (\varepsilon(x) |u(x)|^2 + \mu(x) |v(x)|^2) dx - \int_a^b (u(x) \overline{v'(x)} + v(x) \overline{u'(x)}) dx$$

Let us consider the following decompositions $u(x) = u_1(x) + i u_2(x)$ and $v(x) = v_1(x) + i v_2(x)$ where u_1, u_2, v_1 and v_2 are a real valued functions, we also have

$$-u(x) \overline{v'(x)} - v(x) \overline{u'(x)} = -(u_1 v_1 + u_2 v_2)'(x) - i (u_2 v_1' - u_1 v_2' + v_2 u_1' - v_1 u_2')(x)$$

and we get

$$\begin{aligned} \operatorname{Re}(\mathcal{A}_w(U, U)) &= -\operatorname{Re} \left(\int_a^b u(x) \overline{v'(x)} - v(x) \overline{u'(x)} dx \right) \\ &= - \int_a^b (u_1 v_1 + u_2 v_2)'(x) dx \\ &= u_1(a) v_1(a) + u_2(a) v_2(a) - u_1(b) v_1(b) - u_2(b) v_2(b). \end{aligned}$$

From the same arguments in Sobolev space, there is a constant $\alpha > 0$ such that

$$|u_1(a) v_1(a) + u_2(a) v_2(a) - u_1(b) v_1(b) - u_2(b) v_2(b)| \geq \alpha \left(\|u\|_{\widehat{\mathbf{L}}_2}^2 + \|v\|_{\widehat{\mathbf{L}}_2}^2 \right). \quad (4.17)$$

As a result, there is a constant $\alpha > 0$ such that

$$|\operatorname{Re}(\mathcal{A}_w(U, U))| \geq \alpha \|U\|_{\widehat{\mathbf{L}}_2 \times \widehat{\mathbf{L}}_2}^2, \quad (4.18)$$

where $\|U\|_{\widehat{\mathbf{L}}_2 \times \widehat{\mathbf{L}}_2}^2 = \|u\|_{\widehat{\mathbf{L}}_2}^2 + \|v\|_{\widehat{\mathbf{L}}_2}^2$ and it is obvious to obtain the coercivity bound

$$|\mathcal{A}_w(U, U)| \geq |\operatorname{Re}(\mathcal{A}_w(U, U))| \geq \alpha \|U\|_{\widehat{\mathbf{L}}_2 \times \widehat{\mathbf{L}}_2}^2. \quad (4.19)$$

□

Let w be a real fixed frequency, and denote by \mathcal{H} the subspace of functions $U(\cdot, w) = (u(\cdot, w), v(\cdot, w))$ in $\widehat{\mathbf{H}}_1 \times \widehat{\mathbf{H}}_1$ that satisfy the inequality (4.17).

Hence, from (4.15) and (4.16) the sesquilinear form $\mathcal{A}_w : \mathcal{H} \times \mathcal{H} \rightarrow \mathbb{C}$ is continuous and coercive, and from (4.14) the semi-linear form $\mathcal{L}_w : \mathcal{H} \rightarrow \mathbb{C}$ is continuous.

Now, we can state the following result:

Theorem 4.2. *For a fixed frequency w in \mathbb{R} , then the Lax-Milgram complex version proves that*

1. *The problem (4.5)-(4.6) has a unique solution $U_*(\cdot, w) = (u_*(\cdot, w), v_*(\cdot, w))$ in $\mathcal{H} \subseteq \widehat{\mathbf{H}}_1 \times \widehat{\mathbf{H}}_1$ satisfying*

$$\|U_*(\cdot, w)\|_{\widehat{\mathbf{L}}_2 \times \widehat{\mathbf{L}}_2} \leq \frac{M(w)}{\alpha}, \quad (4.20)$$

where the positive constants α and $M(w)$ are given in (4.17) and (4.14), respectively.

2. *Furthermore, if $\mu, \varepsilon, F(\cdot, w)$ and $G(\cdot, w)$ are in $C([a, b])$, then $U_*(\cdot, w) \in C^1([a, b]) \times C^1([a, b])$ is the unique solution of the problem (4.5)-(4.6) in the usual sense.*

Proof. 1. From (4.15) and (4.16) the sesquilinear form $\mathcal{A}_w : \mathcal{H} \times \mathcal{H} \rightarrow \mathbb{C}$ is continuous and coercive, and from (4.14) the semi-linear form $\mathcal{L}_w : \mathcal{H} \rightarrow \mathbb{C}$ is continuous, thus by using the complex version of Lax-Milgram theorem [4,20], imply that there exists a unique solution $U_*(., w) = (u_*(., w), v_*(., w))$ of the variational problem (4.7) in $\widehat{H}_1 \times \widehat{H}_1$. Since the problem (4.5)-(4.6) is equivalent to the variational formulation problem (4.7), then $U_*(., w) = (u_*(., w), v_*(., w))$ is also the unique weak solution of the problem (4.5)-(4.6). From the continuity of the operator \mathcal{L}_w and the coercivity of the operator \mathcal{A}_w , we have

$$\alpha \|U_*(., w)\|_{\widehat{E}}^2 \leq |\mathcal{A}_w(u_*(., w), u_*(., w))| \leq M(w) \|U_*(., w)\|_{\widehat{E}}.$$

Thus, we obtain the inequality bound (4.20).

Since $\varepsilon, \mu \in L^\infty([a, b], \mathbb{R})$ and $(u_*(., w), v_*(., w)) \in \widehat{H}_1 \times \widehat{H}_1$, then $\varepsilon u_*(., w) \in \widehat{L}_2$ and $\mu v_*(., w) \in \widehat{L}_2$. We have $F(., w) \in \widehat{L}_2$ and $G(., w) \in \widehat{L}_2$, hence

$$\begin{cases} \frac{\partial u_*(., w)}{\partial x} = F(., w) - i w \varepsilon(.) u_*(., w) \in \widehat{L}_2, \\ \frac{\partial v_*(., w)}{\partial x} = G(., w) - i w \mu(.) v_*(., w) \in \widehat{L}_2. \end{cases} \quad (4.21)$$

It follows that $u_*(., w)$ and $v_*(., w)$ belongs to \widehat{H}_1 .

In conclusion, the function $U_*(., w) = (u_*(., w), v_*(., w))$ belongs to \widehat{E} .

2. In the distribution sense, we have that

$$\begin{cases} \frac{\partial u_*(x, w)}{\partial x} = F(x, w) - i w \varepsilon(x) u_*(x, w), \\ \frac{\partial v_*(x, w)}{\partial x} = G(x, w) - i w \mu(x) v_*(x, w). \end{cases} \quad (4.22)$$

for all $x \in [a, b]$. From the Sobolev injection, the functions $u_*(., w)$ and $v_*(., w)$ are in $C([a, b])$ and by hypothesis $\mu, \varepsilon, F(., w)$ and $G(., w)$ are in $C([a, b])$, then from (4.22) the weak solution $U_*(., w) = (u_*(., w), v_*(., w))$ of the problem (4.5)-(4.6) belongs to $C^1([a, b]) \times C^1([a, b])$ and is the unique solution of Problem (4.5)-(4.6) in the usual sense (see also, [5,20]). \square

4.3. γ -Splines finite element approximation

We develop a smooth approximate solution of the Maxwell's wave equations (4.5)-(4.6) in frequency domain using the γ -spline functions. For this purpose, we discretize the interval $[a, b]$ using equally spaced knots $x_i = a + ih, i = 0, 1, 2, \dots, n, x_0 = a, x_n = b$ and $h = (b - a)/n$. For $i = -\gamma, \dots, n + 1$, let us consider a partition of $(n + \gamma + 2)$ nodes of the interval $[a - \gamma h, b + h]$:

$$x_{-\gamma} < \dots < x_{-1} < a = x_0 < x_1 < \dots < x_{n-1} < b = x_n < x_{n+1}, \quad (4.23)$$

For a fixed frequency w in \mathbb{R} , let us denote by \widehat{V}_h^γ the finite dimensional subspace of \widehat{H}_1 , given by

$$\widehat{V}_h^\gamma = \{u_h(., w) \in \widehat{H}_1 : u_h(., w)|_{J_i} \in \mathbb{P}_\gamma; \text{ for } -\gamma \leq i \leq n - 1\}, \quad (4.24)$$

where \mathbb{P}_γ is the vector space of polynomials of degree $\leq \gamma$ and $J_i = [x_i, x_{i+1}]$ for all $-\gamma \leq i \leq n + 1$. It is well known that the dimension of the subspace \widehat{V}_h^γ is $N_\gamma = n + \gamma + 2$.

We use the classical γ -Splines functions as a basis $\{B_1, \dots, B_{N_\gamma}\}$ of the subspace \widehat{V}_h^γ . Here, $(B_i)_{1 \leq i \leq N_\gamma}$ denote the Splines associated to the partition given in (4.23). So, we have

$$B_i(x) = \mathbf{B}_\gamma \left(\frac{x - x_{i-\gamma-1}}{h} \right), \quad i = 1, \dots, N_\gamma, \quad (4.25)$$

where $x_{i-\gamma-1} = a + (i - \gamma - 1)h$ for $i = 1, \dots, N_\gamma$, and \mathbf{B}_γ is the γ -Spline with the support $[0, \gamma + 1]$. We recall that the γ -spline functions \mathbf{B}_γ are computed by using the relationship Eq.(3.3).

The classical Galerkin approximation consists of finding an approximation $(u_h(\cdot, w), v_h(\cdot, w))$ of the exact solution $(u_*(\cdot, w), v_*(\cdot, w))$ as a solution in $\widehat{\mathbb{V}}_h^\gamma \times \widehat{\mathbb{V}}_h^\gamma$ of the following discrete variational problems:

$$\begin{cases} \mathcal{A}_w(u_h(\cdot, w), \varphi_h) + \mathcal{C}(v_h(\cdot, w), \varphi_h) = \mathcal{J}_w(\varphi_h), & \forall \varphi_h(\cdot, w) \in \widehat{\mathbb{V}}_h^\gamma \\ \mathcal{B}_w(v_h(\cdot, w), \theta_h) + \mathcal{C}(u_h(\cdot, w), \theta_h) = \mathcal{K}_w(\theta_h), & \forall \theta_h(\cdot, w) \in \widehat{\mathbb{V}}_h^\gamma \end{cases} \quad (4.26)$$

The solution $(u_h(\cdot, w), v_h(\cdot, w)) \in \widehat{\mathbb{V}}_h^\gamma \times \widehat{\mathbb{V}}_h^\gamma$ of the problem (4.26) is written in the following form:

$$u_h(x, w) = \sum_{i=1}^{N_\gamma} z_{hi}(w) B_i(x) \quad \text{and} \quad v_h(x, w) = \sum_{i=1}^{N_\gamma} \tilde{z}_{hi}(w) B_i(x) \quad (4.27)$$

where the $z_{hi}(w)$ and $\tilde{z}_{hi}(w)$ are unknown complex coefficients depending on the frequency w . By using the test functions $(\varphi_h, \theta_h) = (B_k, B_\ell)$ in the weak discrete variational formulation (4.26), we obtain

$$\begin{cases} \sum_{i=1}^{N_\gamma} z_{hi}(w) \mathcal{A}_w(B_i, B_k) + \sum_{i=1}^{N_\gamma} \tilde{z}_{hi}(w) \mathcal{C}(B_i, B_k) = \mathcal{J}_w(B_k), & k = 1, \dots, N_\gamma, \\ \sum_{i=1}^{N_\gamma} \tilde{z}_{hi}(w) \mathcal{B}_w(B_i, B_\ell) + \sum_{i=1}^{N_\gamma} z_{hi}(w) \mathcal{C}(B_i, B_\ell) = \mathcal{K}_w(B_\ell), & \ell = 1, \dots, N_\gamma, \end{cases} \quad (4.28)$$

with

$$\begin{aligned} \mathcal{A}_w(B_i, B_k) &= i w \int_a^b \varepsilon(x) B_i(x) B_k(x) dx, & \mathcal{C}(B_j, B_k) &= -\frac{1}{h} \int_a^b B_j(x) B'_k(x) dx \\ \mathcal{B}_w(B_j, B_\ell) &= i w \int_a^b \mu(x) B_j(x) B_\ell(x) dx, & \mathcal{C}(B_i, B_\ell) &= -\frac{1}{h} \int_a^b B_i(x) B'_\ell(x) dx \end{aligned}$$

and $\mathcal{J}_w(B_k) = \int_a^b F(x, w) B_k(x) dx - H_b(w) B_k(b) - H_a(w) B_k(a)$, and $\mathcal{K}_w(B_\ell) = \int_a^b G(x, w) B_\ell(x) dx - G_b(w) B_\ell(b) - G_a(w) B_\ell(a)$, for all $(i, j, k, \ell) \in \{1, \dots, N_\gamma\}^4$. Let $A(w) = [A_{ij}(w)]$ be the $N_\gamma \times N_\gamma$ matrix whose entries are the complex coefficients $A_{ik}(w) = \mathcal{A}_w(B_i, B_k)$, $B(w) = [B_{ij}(w)]$ be the $N_\gamma \times N_\gamma$ matrix whose entries are the complex coefficients $B_{j\ell}(w) = \mathcal{B}_w(B_j, B_\ell)$, $C = [C_{i\ell}]$ be the $N_\gamma \times N_\gamma$ matrix whose entries are the complex coefficients $C_{i\ell} = \mathcal{C}(B_i, B_\ell)$, let $\mathbf{b}(w) = (b_1(w), \dots, b_{N_\gamma}(w))^T$ be the complex vector whose coefficients are $b_j(w) = \mathcal{J}_w(B_k)$ and $\tilde{\mathbf{b}}(w) = (\tilde{b}_1(w), \dots, \tilde{b}_{N_\gamma}(w))^T$ be the complex vector whose coefficients are $\tilde{b}_j(w) = \mathcal{K}_w(B_\ell)$ and let $\mathbf{z}_h(w) = (z_{h1}(w), \dots, z_{hN_\gamma}(w))^T$ be the vector of the unknown complex coefficients and $\tilde{\mathbf{z}}_h(w) = (\tilde{z}_{h1}(w), \dots, \tilde{z}_{hN_\gamma}(w))^T$ be the vector of the unknown complex coefficients. For $(i, j) \in \{1, \dots, N_\gamma\}^2$, it is easy to obtain

$$\begin{aligned} A_{ik}(w) &= i w h \int_0^n \varepsilon(a + sh) \mathbf{B}_\gamma(s - i + \gamma + 1) \mathbf{B}_\gamma(s - k + \gamma + 1) ds \\ B_{j\ell}(w) &= i w h \int_0^n \mu(a + sh) \mathbf{B}_\gamma(s - j + \gamma + 1) \mathbf{B}_\gamma(s - \ell + \gamma + 1) ds \\ C_{i\ell} &= - \int_0^n \mathbf{B}_\gamma(s - i + \gamma + 1) \mathbf{B}'_\gamma(s - \ell + \gamma + 1) ds \end{aligned}$$

and

$$\begin{aligned} b_k(w) &= h \int_0^n F(a+sh, w) \mathbf{B}_\gamma(s-k+\gamma+1) ds \\ &\quad - H_b(w) \mathbf{B}_\gamma(n-k+\gamma+1) - H_a(w) \mathbf{B}_\gamma(-k+\gamma+1) \\ \tilde{b}_\ell(w) &= h \int_0^n G(a+sh, w) \mathbf{B}_\gamma(s-\ell+\gamma+1) ds \\ &\quad - G_b(w) \mathbf{B}_\gamma(n-\ell+\gamma+1) - G_a(w) \mathbf{B}_\gamma(-\ell+\gamma+1) \end{aligned}$$

The relations (4.28) leads to the following $2N_\gamma \times 2N_\gamma$ linear system

$$\begin{cases} \mathbf{A}(w) z_h(w) + \mathbf{C} \tilde{z}_h(w) = \mathbf{b}(w) \\ \mathbf{B}(w) \tilde{z}_h(w) + \mathbf{C} z_h(w) = \tilde{\mathbf{b}}(w) \end{cases} \quad (4.29)$$

which is equivalent to the following system of matrices by blocks

$$\begin{pmatrix} \mathbf{A}(w) & \mathbf{C} \\ \mathbf{C} & \mathbf{B}(w) \end{pmatrix} \begin{pmatrix} z_h(w) \\ \tilde{z}_h(w) \end{pmatrix} = \begin{pmatrix} \mathbf{b}(w) \\ \tilde{\mathbf{b}}(w) \end{pmatrix} \quad (4.30)$$

The block matrix $\mathbf{M} = \begin{pmatrix} \mathbf{A}(w) & \mathbf{C} \\ \mathbf{C} & \mathbf{B}(w) \end{pmatrix}$ is also called the assembly matrix or the stiffness matrix, and is the outcome of the discrete variational problem (4.26). For every frequency value w , the coefficients $z_{hk}(w)$ and $\tilde{z}_{h\ell}(w)$ appearing in the expressions (4.27) of the computed solution (u_h, v_h) are obtained by solving the linear system (4.30).

5. Quadrature computations for time-dependent solutions

In the following of this section, an approximate solution $\Phi_h = (\phi_h, \psi_h)$ of the analytic solution $\Phi_* = (\phi_*, \psi_*)$ is calculated as the IFT of $U_h = (u_h, v_h)$. Therefore, we want to use the Gauss-Hermite quadrature method, Rectangle's quadrature, Trapezoidal formula, and Simpson's quadrature methods to compute the IFT of (u_h, v_h) .

Theorem 5.1. *For a fixed time $t \in [t_o, t_o + T]$, the one-dimensional Maxwell problem (2.1)-(2.3) has a unique solution $\Phi(\cdot, t) = (\phi(\cdot, t), \psi(\cdot, t))$, belongs to the space $\mathbf{H}_1 \times \mathbf{H}_1$, obtained as the IFT of the unique solution $U(\cdot, w) = (u(\cdot, w), v(\cdot, w))$ of the problem (4.5)-(4.6); and it is given by*

$$\begin{aligned} \phi(x, t) &= \frac{1}{\sqrt{2\pi}} \int_{-\infty}^{+\infty} u(x, w) e^{itw} dw, \\ \psi(x, t) &= \frac{1}{\sqrt{2\pi}} \int_{-\infty}^{+\infty} v(x, w) e^{itw} dw, \end{aligned} \quad (5.1)$$

for all $x \in [a, b]$.

Proof. This result is an immediate consequence of Theorem 4.2, for further details we refer for instance to [1]. \square

An approximate solution $\Phi_h(\cdot, t) = (\phi_h(\cdot, t), \psi_h(\cdot, t))$ of the 1D-time-dependent Maxwell problem (2.1)-(2.3), is obtained by using the IFT similarly to (5.1),

$$\phi_h(x, t) = \frac{1}{\sqrt{2\pi}} \int_{-\infty}^{+\infty} u_h(x, w) e^{itw} dw \quad \text{and} \quad \psi_h(x, t) = \frac{1}{\sqrt{2\pi}} \int_{-\infty}^{+\infty} v_h(x, w) e^{itw} dw.$$

Consider the finite-dimensional vector space \mathbb{V}_h^γ with dimension N given by

$$\mathbb{V}_h^\gamma = \left\{ \phi_h(\cdot, t) \in \mathbb{H}_1 : \phi_h(\cdot, t)|_{\mathcal{J}_i} \in \mathbb{P}_\gamma; \text{ for } 0 \leq i \leq n-1 \right\}$$

which is spanned by the system $\{B_1, \dots, B_{N_\gamma}\}$. The approximate solution $\Phi_h(\cdot, t) = (\phi_h(\cdot, t), \psi_h(\cdot, t))$ belongs to the space $\mathbb{V}_h^\gamma \times \mathbb{V}_h^\gamma$, and it's given by

$$\Phi_h(x, t) = (\phi_h(x, t), \psi_h(x, t)) = \left(\sum_{i=1}^{N_\gamma} \xi_{h,i}(t) B_i(x), \sum_{j=1}^{N_\gamma} \zeta_{h,j}(t) B_j(x) \right) \quad (5.2)$$

for all $(x, t) \in [a, b] \times [t_0; t_0 + T]$, where the functions $\xi_{h,i}(t)$ and $\zeta_{h,j}(t)$ are respectively the inverse Fourier transform of the coordinates functions $z_{h,i}$ and $\tilde{z}_{h,j}$ solutions of the system (4.30). So, we recall that $\xi_{h,i}(t)$ and $\zeta_{h,j}(t)$ are given as

$$\xi_{h,i}(t) = \frac{1}{\sqrt{2\pi}} \int_{-\infty}^{+\infty} z_{h,i}(w) e^{itw} dw \quad \text{and} \quad \zeta_{h,j}(t) = \frac{1}{\sqrt{2\pi}} \int_{-\infty}^{+\infty} \tilde{z}_{h,j}(w) e^{itw} dw,$$

respectively.

When the signals $\phi(x, \cdot)$ and $\psi(x, \cdot)$ are a fast decay functions or $\phi(x, \cdot)$ and $\psi(x, \cdot)$ are in the Schwartz space $\mathcal{S}(\mathbb{R})$ with respect to the time variable, then we use the Gauss-Hermite quadrature to compute the approximate solution $\Phi_h = (\phi_h, \psi_h)$ of the analytic solution $\Phi_* = (\phi_*, \psi_*)$ (for more detail see [1,2]).

Denote $\varphi_i(w, t) = \frac{1}{\sqrt{2\pi}} e^{(w^2+itw)} z_{h,i}(w)$ and $\tilde{\varphi}_i(w, t) = \frac{1}{\sqrt{2\pi}} e^{(w^2+itw)} \tilde{z}_{h,i}(w)$, then for every $1 \leq i \leq N$, we have

$$\xi_{h,i}(t) = \int_{-\infty}^{+\infty} \varphi_i(w, t) e^{-w^2} dw \quad \text{and} \quad \zeta_{h,i}(t) = \int_{-\infty}^{+\infty} \tilde{\varphi}_i(w, t) e^{-w^2} dw. \quad (5.3)$$

To calculate the integrals given in (5.3), we employ the Gauss-Hermite quadrature formula:

$$(\xi_{h,i}(t), \zeta_{h,i}(t)) \simeq \left(\sum_{\ell=0}^m \alpha_\ell \varphi_i(w_\ell, t), \sum_{\ell=0}^m \alpha_\ell \tilde{\varphi}_i(w_\ell, t) \right), \quad (5.4)$$

where the nodes $(w_\ell)_{0 \leq \ell \leq m}$ are the zeros of the Hermite polynomial \mathcal{H}_{m+1} of degree $m+1$, and the weight coefficients $(\alpha_\ell)_{0 \leq \ell \leq m}$ are given by the Christoffel-Darboux formula [1]. Finally, we get

$$\begin{aligned} \phi_h(x, t) &\simeq \sum_{i=1}^{N_\gamma} \left(\sum_{\ell=0}^m \alpha_\ell \varphi_i(w_\ell, t) \right) B_i(x) = \sum_{\ell=0}^m \alpha_\ell \left(\sum_{i=1}^{N_\gamma} \varphi_i(w_\ell, t) B_i(x) \right), \\ \psi_h(x, t) &\simeq \sum_{i=1}^{N_\gamma} \left(\sum_{\ell=0}^m \alpha_\ell \tilde{\varphi}_i(w_\ell, t) \right) B_i(x) = \sum_{\ell=0}^m \alpha_\ell \left(\sum_{i=1}^{N_\gamma} \tilde{\varphi}_i(w_\ell, t) B_i(x) \right). \end{aligned}$$

And, for other functions, we use other quadrature methods to compute the coefficients $\xi_{h,i}(t)$ and $\zeta_{h,i}(t)$. Let $w_{\max} = \frac{m}{T}$ be the Nyquist critical frequency, we discretize the interval $[-\frac{1}{2} w_{\max}, \frac{1}{2} w_{\max}]$ using equally spaced knots $w_k = -\frac{1}{2} w_{\max} + k \Delta w$, $k = 0, 1, 2, \dots, m$, $w_0 = -\frac{1}{2} w_{\max}$, $w_m = \frac{1}{2} w_{\max}$ and $\Delta w = \frac{1}{T}$. Let use $\delta_{h,i}(t) = \xi_{h,i}(t)$ or $\zeta_{h,j}(t)$, then to compute numerically the functions $\xi_{h,i}(t)$ and $\zeta_{h,j}(t)$, we use the following approach

$$\delta_{h,i}(t) = \frac{1}{\sqrt{2\pi}} \int_{-\infty}^{+\infty} \sigma_{h,i}(w) e^{itw} dw \approx \frac{1}{\sqrt{2\pi}} \int_{-\frac{1}{2} w_{\max}}^{\frac{1}{2} w_{\max}} \sigma_{h,i}(w) e^{itw} dw \quad (5.5)$$

where $\sigma_{h,i}(w) = z_{h,i}(w)$ or $\tilde{z}_{h,i}(w)$ for $1 \leq i \leq N_\gamma$. To solve the problem of functions which have a very oscillating structure and to obtain a sufficiently precise approximate value of the inverse Fourier transform integral, it's essential to provide a very large number m of quadrature nodes.

6. Convergence analysis and error estimate

In the following of this section, we furnish some relevant results on the error estimates. As in [1,2], we consider the Schwartz space $\mathcal{S}(\mathbb{R}; L_2)$ with the topology is endowed by a semi-norms family. The space $\mathcal{S}'(\mathbb{R}; L_2)$ of the tempered distributions, namely the linear and continuous forms from $\mathcal{S}(\mathbb{R}; L_2)$ into \mathbb{R} is the topological dual of the space $\mathcal{S}(\mathbb{R}; L_2)$. For every $s \in \mathbb{R}$, the space $H^s(\mathbb{R}; \mathbb{R})$ given by

$$H^s(\mathbb{R}; \mathbb{R}) = \{\varphi \in \mathcal{S}'(\mathbb{R}; \mathbb{R}) : \widehat{\varphi} \in L_{loc}^2(\mathbb{R}; \mathbb{C}) \text{ and } \int_{-\infty}^{+\infty} (1 + w^2)^s |\widehat{\varphi}(\cdot, w)|^2 dw < \infty\}, \quad (6.1)$$

are endowed with the topology defined by the norm given by

$$\|\varphi\|_{H^s(\mathbb{R}; \mathbb{R})} = \left(\int_{-\infty}^{+\infty} (1 + w^2)^s |\widehat{\varphi}(\cdot, w)|^2 dw \right)^{\frac{1}{2}}. \quad (6.2)$$

The non-homogeneous Sobolev spaces $H^s(\mathbb{R}; L_2)$ given by

$$H^s(\mathbb{R}; L_2) = \{\varphi \in \mathcal{S}'(\mathbb{R}; L_2) : \widehat{\varphi} \in L_{loc}^2(\mathbb{R}; \widehat{L}_2) \text{ and } \int_{-\infty}^{+\infty} (1 + w^2)^s \|\widehat{\varphi}(\cdot, w)\|_{\widehat{L}_2}^2 dw < \infty\} \quad (6.3)$$

are endowed with the topology defined by the norm given by

$$\|\varphi\|_{H^s(\mathbb{R}; L_2)} = \left(\int_{-\infty}^{+\infty} (1 + w^2)^s \|\widehat{\varphi}(\cdot, w)\|_{\widehat{L}_2}^2 dw \right)^{\frac{1}{2}}, \quad (6.4)$$

are Hilbert spaces.

Let $(x_i)_{0 \leq i \leq n}$ be the partition of the interval $[a, b]$ given in (4.23), where $x_0 = a$, $x_n = b$ and $h = (b-a)/n$ is the step size of this partition. Consider the following subspace $\widehat{\mathcal{S}}_h^\gamma$ of $\widehat{\mathcal{V}}_h^\gamma$, given by

$$\widehat{\mathcal{S}}_h^\gamma = \{u_h \in C^1([a, b]) : u_h|_{[x_i, x_{i+1}]} \in \mathbb{P}_\gamma ; \text{ for } -\gamma \leq i \leq n-1\}. \quad (6.5)$$

Let $\mathcal{J}_h^\gamma : \widehat{\mathbf{H}}_1 \rightarrow \widehat{\mathcal{S}}_h^\gamma$ be the interpolating operator such that for every $u \in \widehat{\mathbf{H}}_1$, the function $\mathcal{J}_h^\gamma u$ is the unique γ -spline in $\widehat{\mathcal{S}}_h^\gamma$ satisfying the following interpolating conditions $\mathcal{J}_h^\gamma u(x_i) = u(x_i)$, $i = 0, \dots, n$, together with the further boundary conditions $(\mathcal{J}_h^\gamma u)'(a) = u'(a)$ and $(\mathcal{J}_h^\gamma u)'(b) = u'(b)$.

The γ -spline $\mathcal{J}_h^\gamma u$ could be written as $\mathcal{J}_h^\gamma u(x) = \sum_{i=1}^{N_\gamma} \varrho_i B_i(x)$, for all $x \in [a, b]$ where ϱ_i are the interpolating parameters.

Proposition 6.1. *Let u be any function in $\widehat{\mathbf{H}}_1$. Then*

- a) $\|u' - (\mathcal{J}_h^\gamma u)'\|_{\widehat{L}_2} \leq \|u'\|_{\widehat{L}_2}$,
- b) $\|u - \mathcal{J}_h^\gamma u\|_{\widehat{L}_2} \leq \frac{2h}{\pi} \|u'\|_{\widehat{L}_2}$.

Furthermore, if u be in $\widehat{\mathbf{H}}_\gamma$, then we have : $\|u - \mathcal{J}_h^\gamma u\|_{\widehat{L}_2} \leq \left(\frac{2h}{\pi}\right)^{\gamma+1} \|u^{(\gamma)}\|_{\widehat{L}_2}$.

Proof. The results are demonstrated in [17,18] for $u \in C^1([a, b])$, and, by using the closure of $C^1([a, b])$ in $\widehat{\mathbf{H}}_1$ for its topology, we conclude that the result is well for $u \in \widehat{\mathbf{H}}_1$. On other hand the result is also available for $u \in C^\gamma([a, b])$, then we conclude that the result is well for $u \in \widehat{\mathbf{H}}_\gamma$. \square

Lemma 6.2. *For a fixed frequency $w \in \mathbb{R}$. If $U(\cdot, w) = (u(\cdot, w), v(\cdot, w))$ (respectively $U_h(\cdot, w) = (u_h(\cdot, w), v_h(\cdot, w))$) is a solution of the variational problem (4.7)(resp. (4.26)), then*

$$\|U(\cdot, w) - U_h(\cdot, w)\|_{\widehat{L}_2 \times \widehat{L}_2} \leq \frac{c_3}{\alpha} (1 + w^2)^{\frac{1}{2}} \inf_{V_h \in \widehat{\mathcal{E}}_h^\gamma} \|U(\cdot, w) - V_h(\cdot, w)\|_{\widehat{L}_2 \times \widehat{L}_2}$$

where $\widehat{\mathcal{E}}_h^\gamma := \widehat{\mathcal{V}}_h^\gamma \times \widehat{\mathcal{V}}_h^\gamma$, c_3 and α are respectively the constants with respect to the continuity and the coercivity of \mathcal{A}_w given in (4.15) and (4.16).

Proof. This result is a direct consequence of the C ea lemma (see [25]). \square

Now, we will prove the following result.

Theorem 6.3. *Let h be the step size of the partition given in (4.23). We assume that the following hypotheses hold*

1. *The functions μ and ε are in $L^\infty([a, b])$,*
2. *The functions $f, g \in H^1(\mathbb{R}; L_2)$ and the functions $g_a, g_b, h_a, h_b \in H^1(\mathbb{R}, \mathbb{R})$.*

Then we have the following results:

- i. *The functions $\phi_* \in L^2(\mathbb{R}; H_1)$ and $\psi_* \in L^2(\mathbb{R}; H_1)$.*
- ii. *There exists a constant $C_* > 0$ such that*

$$\|U_* - U_h\|_{L^2(\mathbb{R}; \widehat{L}_2 \times \widehat{L}_2)} \leq C_* h \left\| \frac{\partial \Phi_*}{\partial x} \right\|_{H^1(\mathbb{R}; L_2 \times L_2)}. \quad (6.6)$$

- iii. *We have the following error estimates*

$$\|\Phi_* - \Phi_h\|_{L^2(\mathbb{R}; L_2 \times L_2)} = \mathcal{O}(h). \quad (6.7)$$

where $\Phi = (\phi, \psi)$ and $U = (u, v)$.

Proof. i. We have $u_* = \widehat{\phi}_*$ and $v_* = \widehat{\psi}_*$. Since the functions $F(\cdot, w) \in \widehat{L}_2$, $G(\cdot, w) \in \widehat{L}_2$, $u_*(\cdot, w) \in \widehat{H}_1$, $v_*(\cdot, w) \in \widehat{H}_1$ and the functions $\mu, \varepsilon \in L^\infty([a, b])$, we deduce from Relation (4.22) that $\frac{\partial u_*(\cdot, w)}{\partial x}$ and $\frac{\partial v_*(\cdot, w)}{\partial x}$ belongs to \widehat{L}_2 . Now, using the fact that the functions μ and ε are bounded on $[a, b]$ and the inequality $(|a| + |b|)^2 \leq 2(|a|^2 + |b|^2)$, it follows that there exists a constant $C_1 > 0$ such that

$$\begin{aligned} \left| \frac{\partial \widehat{\phi}_*}{\partial x}(x, w) \right|^2 &\leq C_1(1 + w^2) \left(|F(x, w)|^2 + |u_*(x, w)|^2 \right), \\ \left| \frac{\partial \widehat{\psi}_*}{\partial x}(x, w) \right|^2 &\leq C_1(1 + w^2) \left(|G(x, w)|^2 + |v_*(x, w)|^2 \right), \end{aligned}$$

for all $x \in [a, b]$. The Lebesgue theorem of derivation under the integral sign allows to write $\frac{\partial \widehat{\phi}_*}{\partial x}(\cdot, w) = \frac{\partial \phi_*}{\partial x}(\cdot, w)$ and $\frac{\partial \widehat{\psi}_*}{\partial x}(\cdot, w) = \frac{\partial \psi_*}{\partial x}(\cdot, w)$. By integrating over $]a, b[$ in the last inequalities, we obtain

$$\left\| \frac{\partial \widehat{\Phi}_*}{\partial x}(\cdot, w) \right\|_{\widehat{L}_2 \times \widehat{L}_2}^2 \leq C_1(1 + w^2) \left(\|F(\cdot, w)\|_{L_2}^2 + \|G(\cdot, w)\|_{L_2}^2 + \|U_*(\cdot, w)\|_{\widehat{H}_1 \times \widehat{H}_1}^2 \right),$$

where $\frac{\partial \widehat{\Phi}_*}{\partial x} = \left(\frac{\partial \phi_*}{\partial x}, \frac{\partial \psi_*}{\partial x} \right)$.

From Theorem 4.2, we have $\|U_*(\cdot, w)\|_{\widehat{H}_1 \times \widehat{H}_1} \leq \frac{M(w)}{\alpha}$ where $M(w)$ is given in (4.14). It follows that, there exists a constant $C_2 > 0$ such that

$$\begin{aligned} \left\| \frac{\partial \widehat{\Phi}_*}{\partial x}(\cdot, w) \right\|_{\widehat{L}_2 \times \widehat{L}_2}^2 &\leq \frac{C_2(1 + w^2)}{\alpha^2} \left(\|F(\cdot, w)\|_{L_2}^2 + \|G(\cdot, w)\|_{L_2}^2 + |G_a(w)|^2 \right. \\ &\quad \left. + |G_b(w)|^2 + |H_a(w)|^2 + |H_b(w)|^2 \right) \\ &= \frac{C_2(1 + w^2)}{\alpha^2} \left(\|\widehat{f}(\cdot, w)\|_{L_2}^2 + \|\widehat{g}(\cdot, w)\|_{L_2}^2 + |\widehat{g}_a(w)|^2 \right. \\ &\quad \left. + |\widehat{g}_b(w)|^2 + |\widehat{h}_a(w)|^2 + |\widehat{h}_b(w)|^2 \right). \end{aligned}$$

Integrating over \mathbb{R} by taking into account Item 2, we obtain

$$\begin{aligned} \left\| \frac{\partial \Phi_*}{\partial x} \right\|_{L^2(\mathbb{R}; L_2) \times L^2(\mathbb{R}; L_2)}^2 &\leq \frac{C_2}{\alpha^2} (\|f\|_{\widehat{H}^1(\mathbb{R}; L_2)}^2 + \|g\|_{\widehat{H}^1(\mathbb{R}; L_2)}^2 + \|g_a\|_{\widehat{H}^1(\mathbb{R}; \mathbb{R})}^2 \\ &\quad + \|g_b\|_{\widehat{H}^1(\mathbb{R}; \mathbb{R})}^2 + \|h_a\|_{\widehat{H}^1(\mathbb{R}; \mathbb{R})}^2 + \|h_b\|_{\widehat{H}^2(\mathbb{R}; \mathbb{R})}^2) < \infty. \end{aligned}$$

ii. The following bound error is obtained by using Cea's lemma (see [20]). We have

$$\|U_*(\cdot, w) - U_h(\cdot, w)\|_{\widehat{L}_2 \times \widehat{L}_2} \leq \frac{c_3}{\alpha} \sqrt{1 + w^2} \inf_{V_h \in \widehat{E}_h^\gamma} \|U_*(\cdot, w) - V_h(\cdot, w)\|_{\widehat{L}_2 \times \widehat{L}_2}, \quad (6.8)$$

where c_3 and α are the continuity and the coercivity constants given in (4.15) and (4.16), respectively. Since $\mathcal{J}_h^\gamma u_*(\cdot, w)$ and $\mathcal{J}_h^\gamma v_*(\cdot, w)$ belongs to $\widehat{S}_h^\gamma \subset \widehat{V}_h^\gamma$, it follows that,

$$\inf_{V_h \in \widehat{E}_h^\gamma} \|U_*(\cdot, w) - V_h(\cdot, w)\|_{\widehat{L}_2 \times \widehat{L}_2} \leq \|U_*(\cdot, w) - \mathcal{J}_h^\gamma U_*(\cdot, w)\|_{\widehat{L}_2 \times \widehat{L}_2}, \quad (6.9)$$

where $\mathcal{J}_h^\gamma U_*(\cdot, w) = (\mathcal{J}_h^\gamma u_*(\cdot, w), \mathcal{J}_h^\gamma v_*(\cdot, w))$.

Since the solution $U_*(\cdot, w) = (u_*(\cdot, w), v_*(\cdot, w))$ belongs to $\widehat{H}_1 \times \widehat{H}_1$ and according to Proposition 6.1, we obtain

$$\|u_*(\cdot, w) - \mathcal{J}_h^\gamma u_*(\cdot, w)\|_{\widehat{L}_2} \leq \frac{2h}{\pi} \left\| \frac{\partial u_*}{\partial x}(\cdot, w) \right\|_{\widehat{L}_2}, \quad (6.10)$$

and

$$\|v_*(\cdot, w) - \mathcal{J}_h^\gamma v_*(\cdot, w)\|_{\widehat{L}_2} \leq \frac{2h}{\pi} \left\| \frac{\partial v_*}{\partial x}(\cdot, w) \right\|_{\widehat{L}_2}, \quad (6.11)$$

Therefore

$$\|U_*(\cdot, w) - \mathcal{J}_h^\gamma U_*(\cdot, w)\|_{\widehat{L}_2 \times \widehat{L}_2} \leq \frac{2h}{\pi} \left\| \frac{\partial U_*}{\partial x}(\cdot, w) \right\|_{\widehat{L}_2 \times \widehat{L}_2}. \quad (6.12)$$

Using the relations (6.8), (6.9), (6.11) and (6.12) together with the relations $\frac{\partial u_*}{\partial x}(\cdot, w) = \frac{\partial \widehat{\phi}_*}{\partial x}(\cdot, w)$ and $\frac{\partial v_*}{\partial x}(\cdot, w) = \frac{\partial \widehat{\psi}_*}{\partial x}(\cdot, w)$, we get the bound error

$$\|U_*(\cdot, w) - U_h(\cdot, w)\|_{\widehat{L}_2 \times \widehat{L}_2}^2 \leq \left(\frac{2C_1}{\pi\alpha} \right)^2 h^2 (1 + w^2) \left\| \frac{\partial \widehat{\Phi}_*}{\partial x}(\cdot, w) \right\|_{\widehat{L}_2 \times \widehat{L}_2}^2.$$

Integrating over \mathbb{R} with respect to the frequency variable w , we also obtain

$$\|U_* - U_h\|_{L^2(\mathbb{R}; \widehat{L}_2 \times \widehat{L}_2)} \leq C_* h \left\| \frac{\partial \widehat{\Phi}_*}{\partial x} \right\|_{\widehat{H}^1(\mathbb{R}; L_2 \times L_2)}, \text{ and } C_* = \frac{C_1}{\alpha}.$$

iii. Now, by using the Parseval identity, we get

$$\int_{-\infty}^{+\infty} |(\phi_* - \phi_h)(x, t)|^2 dt = \frac{1}{2\pi} \int_{-\infty}^{+\infty} |u_*(x, w) - u_h(x, w)|^2 dw \quad (6.13)$$

and,

$$\int_{-\infty}^{+\infty} |(\psi_* - \psi_h)(x, t)|^2 dt = \frac{1}{2\pi} \int_{-\infty}^{+\infty} |v_*(x, w) - v_h(x, w)|^2 dw. \quad (6.14)$$

Therefore, using the vectorial notation $\Phi = (\phi, \psi)$ and $U = (u, v)$, we obtain

$$\begin{aligned} \int_{-\infty}^{+\infty} \|(\Phi_* - \Phi_h)(x, t)\|^2 dt &= \frac{1}{2\pi} \int_{-\infty}^{+\infty} \left\| \widehat{\Phi}_*(x, w) - \widehat{\Phi}_h(x, w) \right\|^2 dw \\ &= \frac{1}{2\pi} \int_{-\infty}^{+\infty} \|U_*(x, w) - U_h(x, w)\|^2 dw \end{aligned} \quad (6.15)$$

where $\|(\Phi_* - \Phi_h)(x, t)\|^2 = |(\phi_* - \phi_h)(x, t)|^2 + |(\psi_* - \psi_h)(x, t)|^2$ and

$$\|U_*(x, w) - U_h(x, w)\|^2 = |u_*(x, w) - u_h(x, w)|^2 + |v_*(x, w) - v_h(x, w)|^2.$$

Integrating the relations in (6.13) and (6.15) on $[a, b]$ with respect to the variable x and using Fubini's theorem, we get

$$\int_{-\infty}^{+\infty} \|\Phi_*(\cdot, t) - \Phi_h(\cdot, t)\|_{L_2 \times L_2}^2 dt = \frac{1}{2\pi} \int_{-\infty}^{+\infty} \|U_*(\cdot, w) - U_h(\cdot, w)\|_{L_2 \times L_2}^2 dw.$$

It follows that

$$\|\Phi_* - \Phi_h\|_{L^2(\mathbb{R}; L_2 \times L_2)} = \frac{1}{\sqrt{2\pi}} \|U_* - U_h\|_{L^2(\mathbb{R}; \widehat{L}_2 \times \widehat{L}_2)}. \quad (6.16)$$

Now, using the result of Item ii, we obtain the following inequality

$$\|\Phi_* - \Phi_h\|_{L^2(\mathbb{R}; L_2 \times L_2)} \leq \frac{C_*}{\sqrt{2\pi}} h \left\| \frac{\partial \Phi_*}{\partial x} \right\|_{H^1(\mathbb{R}; L_2 \times L_2)},$$

We make this result is proved similarly to the approach of Item 3., which conclude the proof. \square

Theorem 6.4. *Let h be the step size of the partition given in (4.23). We assume that*

1. *The functions μ and ε are in $L^\infty([a, b])$,*
2. *The functions $f, g \in L^2(\mathbb{R}; L_2)$ and the functions $g_a, g_b, h_a, h_b \in L^2(\mathbb{R})$.*

Then we have the following results:

- i. *The function $\frac{\partial \phi_*}{\partial x} \in H^{-1}(\mathbb{R}; L_2)$ and $\frac{\partial \psi_*}{\partial x} \in H^{-1}(\mathbb{R}; L_2)$.*
- ii. *There exists a constant $C_* > 0$ such that*

$$\|\Phi_* - \Phi_h\|_{H^{-1}(\mathbb{R}; L_2 \times L_2)} \leq C_* h \left\| \frac{\partial \Phi_*}{\partial x} \right\|_{L^2(\mathbb{R}; L_2 \times L_2)}. \quad (6.17)$$

where $\Phi_* = (\phi_*, \psi_*)$.

Proof. To prove the result, we use some arguments and consequences of Theorem 6.3. \square

Theorem 6.5. *Let h be the step size of the partition given in (4.23) and the solution $\Phi_* = (\phi_*, \psi_*)$ of the problem (2.1)-(2.3) belong to $H_1 \times H_1$ and satisfies the Theorem 6.3. We assume that the solution (ϕ_*, ψ_*) is in $H_\gamma \times H_\gamma$, then we have the following results:*

- i. *The function $\phi_* \in L^2(\mathbb{R}; H_\gamma)$ and $\psi_* \in L^2(\mathbb{R}; H_\gamma)$.*
- iii. *We have the following convergence order*

$$\|\Phi_* - \Phi_h\|_{L^2(\mathbb{R}; L_2 \times L_2)} = \mathcal{O}(h^{\gamma+1}). \quad (6.18)$$

where $\Phi_h = (\phi_h, \psi_h)$.

Proof. To demonstrates this result, we use some arguments of Proposition 6.1 and consequences of Theorem 6.3. \square

Now, we define the $L^p \times L^p$ relative error function from

$$L^p \times L^p - \text{error} = \frac{\|\Phi_e - \Phi_h\|_{L^p \times L^p}}{\|\Phi_e\|_{L^p \times L^p}}, \quad \text{for } p = 1, 2, \infty$$

where $\|\cdot\|_{L^p \times L^p}$ is the $L^p \times L^p$ -norm, $\Phi_e = (\phi_e, \psi_e)$ and $\Phi_h = (\phi_h, \psi_h)$ are respectively the analytic and computed solutions of the one-dimensional Maxwell's problem (2.1)-(2.3). In summary, the Fourier Transform Discretization based on γ -spline finite element method to solve the one-dimensional Maxwell's problem (2.1)-(2.3) can be realized in the following Algorithm :

Algorithm 1 Fourier Transform Discretization for 1D Maxwell's equations

1: **Forward stage:** Construct the Fourier transforms $u(\cdot, w) = \widehat{\phi}(\cdot, w)$, $v(\cdot, w) = \widehat{\psi}(\cdot, w)$, $G_a(w) = \widehat{g}_a(w)$, $G_b(w) = \widehat{g}_b(w)$, $H_a(w) = \widehat{h}_a(w)$ and $H_b(w) = \widehat{h}_b(w)$ of $\phi(x, \cdot)$, $\psi(x, \cdot)$, g_a , g_b , h_a and h_b according to eq.(4.3).

2: **for each frequency w do**

3: • Form the given γ -spline basis $B_i(x) = B_\gamma\left(\frac{x-x_i-\gamma-1}{h}\right)$ such that

$$u_h(x, \omega) = \sum_{i=1}^{N_\gamma} z_{h,i}(\omega) B_i(x) \quad \text{and} \quad v_h(x, \omega) = \sum_{i=1}^{N_\gamma} \tilde{z}_{h,i}(\omega) B_i(x).$$

4: • Formulate the weak variational formulation Eq.(4.28).

5: • Solve the linear system Eq.(4.30).

6: **end for**

7: **Backward stage:** Using the IFT (5.3) and the quadrature methods (5.4)-(5.5), calculate $\xi_{h,i}(t)$ and $\zeta_{h,i}(t)$ for $i = 1, \dots, N_\gamma$

8: **for** $i = 1, \dots, N_\gamma$ **do compute**

$$\xi_{h,i}(t) = \int_{-\infty}^{+\infty} \varphi_i(w, t) e^{-w^2} dw \quad \text{or} \quad \xi_{h,i}(t) = \frac{1}{\sqrt{2\pi}} \int_{-\frac{1}{2} w_{\max}}^{\frac{1}{2} w_{\max}} z_{h,i}(w) e^{itw} dw$$

$$\zeta_{h,i}(t) = \int_{-\infty}^{+\infty} \psi_i(w, t) e^{-w^2} dw \quad \text{or} \quad \zeta_{h,i}(t) = \frac{1}{\sqrt{2\pi}} \int_{-\frac{1}{2} w_{\max}}^{\frac{1}{2} w_{\max}} \tilde{z}_{h,i}(w) e^{itw} dw$$

9: **for** $t \in [t_o, t_o + T]$ **do compute**

$$\phi_h(x, t) = \sum_{i=1}^{N_\gamma} \xi_{h,i}(t) B_i(x) \quad \text{and} \quad \psi_h(x, t) = \sum_{i=1}^{N_\gamma} \zeta_{h,i}(t) B_i(x)$$

10: **end for**

11: **end for**

12: Error estimate and Convergence Orders:

$$L^p \times L^p - \text{error} := \frac{\|(\phi_e, \psi_e) - (\phi_h, \psi_h)\|_{L^p \times L^p}}{\|(\phi_e, \psi_e)\|_{L^p \times L^p}}, \quad p = 1, 2, \infty.$$

7. Numerical results and order of convergence

We consider six experimental tests to compute the solution of the IFT. Also, we use the quadrature formulae, for example: Gauss-Hermite quadrature, Rectangle's quadrature, Trapezoidal quadrature, Simpson's quadrature, and Gauss quadrature. In the following numerical experiments, we subdivide the time interval $[t_0, t_0 + T]$ into uniform spaced knots $t_k = t_0 + k\Delta t$, for $0 \leq k \leq p$, where the time step size is $\Delta t = \frac{T}{p}$. The solution of the Maxwell's problem considered here is obviously a time-dependent digital signal.

7.1. Time-dependent Harmonic solution of 1D Maxwell's equations

Let ω be a fixed frequency parameter and $(x, t) \in [a, b] \times [t_0, t_0 + T]$, the harmonic state solution of the one-dimensional Maxwell's equations is to find a pair of functions (φ_1, φ_2) depending on the space variable such that

$$\phi_e(x, t) = \varphi_1(x) e^{i\omega t} \quad \text{and} \quad \psi_e(x, t) = \varphi_2(x) e^{i\omega t}$$

are the unique solutions of the Maxwell's equations (2.1) with the boundary conditions (2.3); also equivalently the pair of functions (ϕ, ψ) is the unique solution of the following problem

$$\begin{cases} (i\omega \varepsilon(x) \varphi_1(x) + \varphi_1'(x)) e^{i\omega t} = f(x, t), \\ (i\omega \mu(x) \varphi_2(x) + \varphi_2'(x)) e^{i\omega t} = g(x, t), \\ g_a(t) = -\varphi_1(a) e^{i\omega t}, \quad g_b(t) = \varphi_1(b) e^{i\omega t}, \\ h_a(t) = -\varphi_2(a) e^{i\omega t}, \quad h_b(t) = \varphi_2(b) e^{i\omega t} \end{cases} \quad (7.1)$$

for all $(x, t) \in]a, b[\times [t_0, t_0 + T]$, with the initial conditions $\phi(x, t_0) = \varphi_1(x) e^{i\omega t_0}$ and $\psi(x, t_0) = \varphi_2(x) e^{i\omega t_0}$. So, the functions φ_1 and φ_2 are written in the system spanned by B-spline basis functions as follows

$$\varphi_1(x) = \sum_{i=1}^{N_\gamma} z_{hi} B_i(x) \quad \text{and} \quad \varphi_2(x) = \sum_{i=1}^{N_\gamma} \tilde{z}_{hi} B_i(x) \quad (7.2)$$

From some arguments used in Subsection 4.3, we obtain the following blocks matrices system to solve

$$\begin{pmatrix} i\omega A & C \\ C & i\omega B \end{pmatrix} \begin{pmatrix} z_h \\ \tilde{z}_h \end{pmatrix} = \begin{pmatrix} e^{-i\omega t} b(t) \\ e^{-i\omega t} \tilde{b}(t) \end{pmatrix} \quad (7.3)$$

where A , B and C are the matrices with the coefficients $A_{ij} = \int_a^b \varepsilon(x) B_i(x) B_j(x) dx$, $B_{ij} = \int_a^b \mu(x) B_i(x) B_j(x) dx$ and $C_{ij} = -\int_a^b B_i(x) B_j'(x) dx$ respectively, and $b(t)$ and $\tilde{b}(t)$ are the vectors with the coefficients

$$\begin{aligned} b_j(t) &= \int_a^b f(x, t) B_j(x) dx - h_b(t) B_j(b) - h_a(t) B_j(a) \\ \tilde{b}_j(t) &= \int_a^b g(x, t) B_j(x) dx - g_b(t) B_j(b) - g_a(t) B_j(a) \end{aligned}$$

In this experiment test, we solve the Maxwell's problem (7.1) in harmonic state using magnetic permeability constant μ and electrical permittivity constant ε . The sources terms f and g , the boundary functions g_a, g_b, h_a and h_b and the initial datum ϕ_0 and ψ_0 are calculated such that the analytic solutions of (7.1) are given for every $(x, t) \in [a, b] \times [t_0, t_0 + T]$ by

$$\phi_e(x, t) = A_o e^{i\omega t} \cos(x) \quad \text{and} \quad \psi_e(x, t) = B_o e^{i\omega t} \sin(x).$$

where A_o and B_o are constants.

Table 1: $L^2 \times L^2$ -error depending of the mesh number n for a different γ -splines basis functions and with $A_o = B_o = 1$, $\mu = 10^5$, $\varepsilon = 2 * 10^5$, $\omega = \pi$, $a = -6$, $b = 6$, $t_o = 0$ and $T = 1$.

n	\mathbf{B}_1	\mathbf{B}_2	\mathbf{B}_3	\mathbf{B}_4	\mathbf{B}_5	\mathbf{B}_6
15	2.6595e-2	3.4675e-3	4.7431e-4	6.3229e-5	9.5855e-6	1.3552e-6
30	7.1422e-3	3.9648e-4	2.4712e-5	1.6419e-6	1.1168e-7	7.3056e-9
60	1.7646e-3	5.0092e-5	2.1865e-6	6.3040e-8	1.6370e-9	1.6362e-8
120	4.4851e-4	6.1871e-6	9.5652e-8	2.7003e-8	1.8512e-6	3.7535e-4
160	2.4665e-4	8.2115e-6	3.5126e-8	1.7508e-6	1.0524e-4	1.3709e-2
192	1.4374e-4	3.6217e-6	1.4494e-8	1.1501e-5	1.3022e-3	1.8721e-1

Table 2: Non zeros of sparsity matrix depending on the mesh number n , the γ -splines basis functions and with $A_o = B_o = 1$, $\mu = 10^5$, $\varepsilon = 2 * 10^5$, $\omega = \pi$, $a = -6$, $b = 6$, $t_o = 0$ and $T = 1$.

n	\mathbf{B}_1	\mathbf{B}_2	\mathbf{B}_3	\mathbf{B}_4	\mathbf{B}_5	\mathbf{B}_6
15	156	290	432	582	740	906
30	306	560	822	1092	1370	1656
60	606	1100	1602	2112	2630	3156
120	1206	2180	3162	4152	5150	6156
160	1606	2900	4202	5512	6830	8156
192	1926	3476	5034	6600	8174	9756

In this example, we summarize the errors for harmonic state solutions of 1D Maxwell's equations. We examine the accuracy of the harmonic solution based on the γ -splines concerning the number of evenly spaced knots in the computational domain. We set the knots points number n and $(\mathbf{B}_\gamma)_{1 \leq \gamma \leq 6}$ the γ -splines and we summarize in Table 1 the $L^2 \times L^2$ -error norms at time $t = 1$ using different values of n and different values of the degree γ of splines functions. In Table 1, we observe that the $L^2 \times L^2$ -error norms increases with respect to increasing the degree of the spline γ and the mesh number n , so this is strongly related to the coefficient of the stiffness matrix during the implementation of the solver code. Since a large degree γ of the spline function involved a reduction in the size of the stiffness matrix, which generates a discount in the memory of the computing machine, it's significant to use the smallest knots points number n relatively to a large degree of the spline function. So, the stiffness matrix is sparse, and Table 2 summarizes the sparsity number with respect to the knots points number n and the degree γ of splines functions. For several tests carried out, it is better to use a higher degree γ of the spline function if the domain $[a, b]$ is very large. The CPU times are done in a few milliseconds, and it's observed a slower increase when increasing the mesh number and the degree of a spline.

7.2. Accuracy test for one-dimensional Maxwell's equations

In this numerical test, we solve the Maxwell's problem (2.1)-(2.2)-(2.3) using the magnetic permeability constant μ and the electrical permittivity constant ε . The sources terms f and g , the boundary functions g_a , g_b , h_a and h_b and the initial datum ϕ_0 and ψ_0 are computed such that the analytic solution of the problem (2.1)-(2.2)-(2.3) is given by

$$\phi_e(x, t) = A_o \cos(\pi x) \sin(t) \quad \text{and} \quad \psi_e(x, t) = B_o \sin(\pi x) \cos(t)$$

for all $(x, t) \in [a, b] \times [t_o, t_o + T]$, where A_o and B_o are constants.

In this accuracy test, we solve the Maxwell's problem (2.1)-(2.2)-(2.3) in the domain $[-70, 70] \times [0.5, 1.5]$.

All computations are used with the data $\mu = 10^6$, $\varepsilon = 10^7$, $t_o = 0.5$, $T = 1$ and $A_o = B_o = 1$.

Table 3: L^2 -error for one-dimensional Maxwell's equations using the spline \mathbf{B}_6 .

n	Rectangle Method		Trapeze Method		Simpson Method		Gauss-Hermite Method	
	L^2 -error	CPU	L^2 -error	CPU	L^2 -error	CPU	L^2 -error	CPU
50	1.8254e-01	2.16	1.8254e-01	3.06	1.8203e-01	1.91	2.1186e-01	1.72
100	1.4914e-04	3.69	1.4914e-04	5.81	1.4914e-04	3.10	1.4838e-04	2.94
200	3.9392e-07	6.64	3.8478e-07	10.1	3.8674e-07	5.81	3.8922e-07	5.67
400	1.4989e-09	12.6	1.4989e-09	19.9	1.4989e-09	11.4	1.6628e-09	11.2
800	2.7170e-08	25.6	2.7167e-08	41.1	2.7170e-08	23.8	5.4488e-08	24.6

Table 4: L^2 -error for one-dimensional Maxwell's equations using the spline \mathbf{B}_3 .

n	Rectangle Method		Trapeze Method		Simpson Method		Gauss-Hermite Method	
	L^2 -error	CPU	L^2 -error	CPU	L^2 -error	CPU	L^2 -error	CPU
50	3.3867e-01	1.60	3.3867e-01	2.80	1.9660e-01	1.39	1.9660e-01	1.57
100	8.0655e-03	3.13	8.0655e-03	5.17	7.9204e-03	2.87	7.9204e-03	2.94
200	3.6816e-04	5.91	3.6816e-04	10.1	3.6026e-04	5.58	3.6026e-04	5.71
400	2.1056e-05	11.8	2.1056e-05	19.5	2.0605e-05	11.3	2.0605e-05	11.4
800	1.2882e-06	24.7	1.2882e-06	39.5	1.2628e-06	22.1	1.2696e-06	24.8

Table 5: L^2 -error for one-dimensional Maxwell's equations using the spline \mathbf{B}_1 .

n	Rectangle Method		Trapeze Method		Simpson Method		Gauss-Hermite Method	
	L^2 -error	CPU	L^2 -error	CPU	L^2 -error	CPU	L^2 -error	CPU
50	3.8747e-01	1.84	3.8747e-01	2.70	3.8747e-01	1.53	3.8747e-01	1.54
100	1.6862e-01	3.17	1.6862e-01	5.23	1.6862e-01	2.69	1.6862e-01	2.67
200	4.1202e-02	5.85	4.1202e-02	9.93	4.1202e-02	5.18	4.1202e-02	5.24
400	1.0218e-02	12.1	1.0218e-02	19.0	1.0218e-02	10.3	1.0218e-02	10.3
800	2.5508e-03	23.3	2.5508e-03	39.3	2.5508e-03	21.8	2.5508e-03	22.2

This example aims to compute the relative errors in the frequency approach method with the quadrature computations based on the Rectangle's Method, Trapezoidal Method, Simpson Method, and Gauss-Hermite Method. We consider the relative $L^p \times L^p$ -norm error function defined as

$$L^p \times L^p - \text{norm error} = \frac{\|(\phi_e, \psi_e) - (\phi_h, \psi_h)\|_{L^p \times L^p}}{\|(\phi_e, \psi_e)\|_{L^p \times L^p}}, \quad (7.4)$$

where $\|\cdot\|_{L^p \times L^p}$ is the $L^p \times L^p$ -norm, $\Phi_h = (\phi_h, \psi_h)$ and $\Phi_e = (\phi_e, \psi_e)$ are respectively, the computed and analytic solutions. Since the considered solutions ϕ_e and ψ_e are real-valued functions, then only real parts of the solutions are considered. Thus, we check the accuracy of the Fourier Transform Discretization concerning the number of knots points employed in the computational domain. To this end we summarize in Tables 3, 4 and 5 the $L^2 \times L^2$ -error norm at time $t = 1$ using different values of n and the quadrature computations are based on Rectangle's Method, Trapezoidal Method, Simpson Method and Gauss-Hermite Method. It is obvious that increasing the number of knots points in the computational domain results in a decrease in all error norms along with an increase in the computational cost. Like features have been observed for other simulations, not reported here, with the $L^\infty \times L^\infty$ -error and the $L^1 \times L^1$ -error norms for other splines \mathbf{B}_2 , \mathbf{B}_4 and \mathbf{B}_5 . It should be stressed that the leading part of the

CPU times listed in all Tables 3, 4 and 5 is used by the direct solver for solving the associated linear systems. All the quadrature methods considered here to compute the IFT give outstanding results. This is quite remarkable in the numerical tests illustrated in the tables 3, 4 and 5. Similarly, it's well noted that other results are observed for other simulations with other splines \mathbf{B}_2 , \mathbf{B}_4 , and \mathbf{B}_5 .

7.3. Rastrigin solutions for one-dimensional Maxwell's equations

The source terms f and g , the boundary functions g_a, g_b, h_a, h_b and the initial datum ϕ_0 and ψ_0 are calculated such that the analytic solutions of the Maxwell's equations (2.1) with the boundary conditions (2.3) are the Rastrigin functions given by

$$\begin{aligned}\phi_e(x, t) &= 8t^2 + 8x^2 - 10(\cos(4\pi t) + \cos(8\pi x)) \\ \psi_e(x, t) &= 8t^2 + 8x^2 + 10(\sin(4\pi t) + \sin(8\pi x))\end{aligned}$$

for all $(x, t) \in [a, b] \times [t_o, t_o + T]$. We use the Rastrigin functions as a solutions of 1D Maxwell's equations to see the performance and ability of our Algorithm 1.

In Figure 2, we give a plot of exact and computed solutions. The first column and the second column illustrate respectively the plot of the solutions $(x, t) \mapsto \phi(x, t)$ and $(x, t) \mapsto \psi(x, t)$, for all $(x, t) \in [-1, 1] \times [1, 2]$. On the right-row of Fig. 2 and on the left-row of Fig. 2, we give the plot of the relative errors considered as a functions $E_{\phi, h} : t \in [t_o, t_o + T] \mapsto E_{\phi, h}(t)$ and $E_{\psi, h} : t \in [t_o, t_o + T] \mapsto E_{\psi, h}(t)$ respectively, where

$$E_{\theta, h}(t) = \left(\left(\sum_{i=1}^n |\theta_e(x_i, t) - \theta_h(x_i, t)| \right) / \left(\sum_{i=1}^n |\theta_e(x_i, t)| \right) \right)^{1/2} \quad \text{for } \theta = \phi \text{ or } \psi$$

7.4. Verification test for one-dimensional Maxwell's equations

Now, we consider the Maxwell's equations (2.1) with the boundary conditions (2.3). We can still solve it using a discontinuity jump in the magnetic permeability μ and in the electrical permittivity ε coefficients given as a function, for example, by the restrictive piecewise values in Table 6.

Table 6: Values of μ and ε for different subsets of $[a, b]$ in this verification test problem.

	$[a, \frac{3a+b}{4}[$	$[\frac{3a+b}{4}, \frac{a+b}{2}[$	$[\frac{a+b}{2}, \frac{a+3b}{4}[$	$[\frac{a+3b}{4}, b]$
Permeability μ	μ_1	μ_2	μ_3	μ_4
Permittivity ε	ε_1	ε_2	ε_3	ε_4

For the piecewise magnetic permeability μ and the piecewise electrical permittivity ε functions, we solve the system Maxwell's equations (2.1) with the boundary conditions (2.3) subject to spatially bounded sources f and g defined by $f(x, t) = 10$ and $g(x, t) = 1$ for $t \in [t_o, t_o + T]$, respectively.

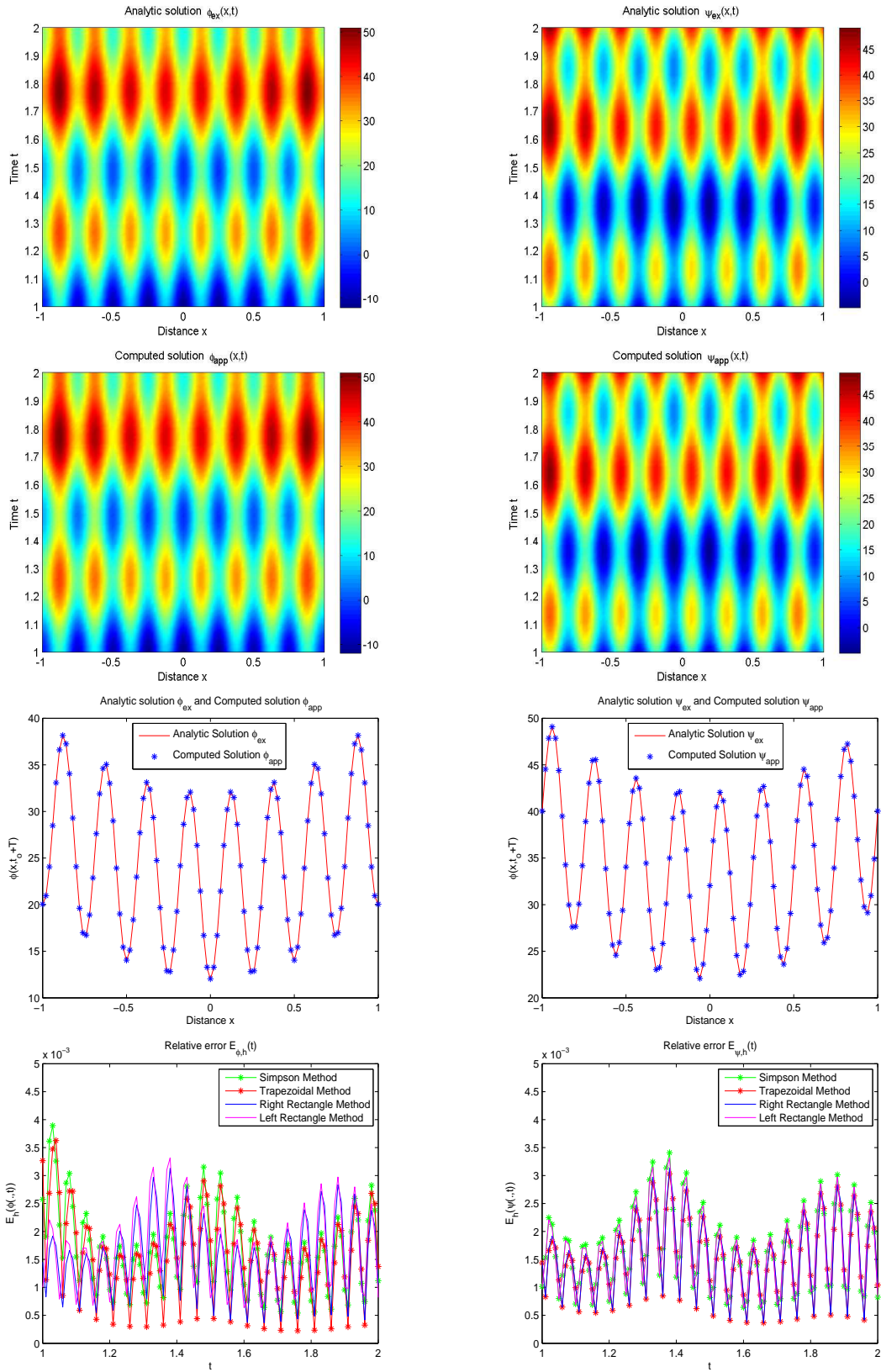


Figure 2: Rastrigin solutions to 1D Maxwell's equations are plotted: the scalar flux ϕ_{B_γ} (left column) and the scalar flux ψ_{B_γ} (right column).

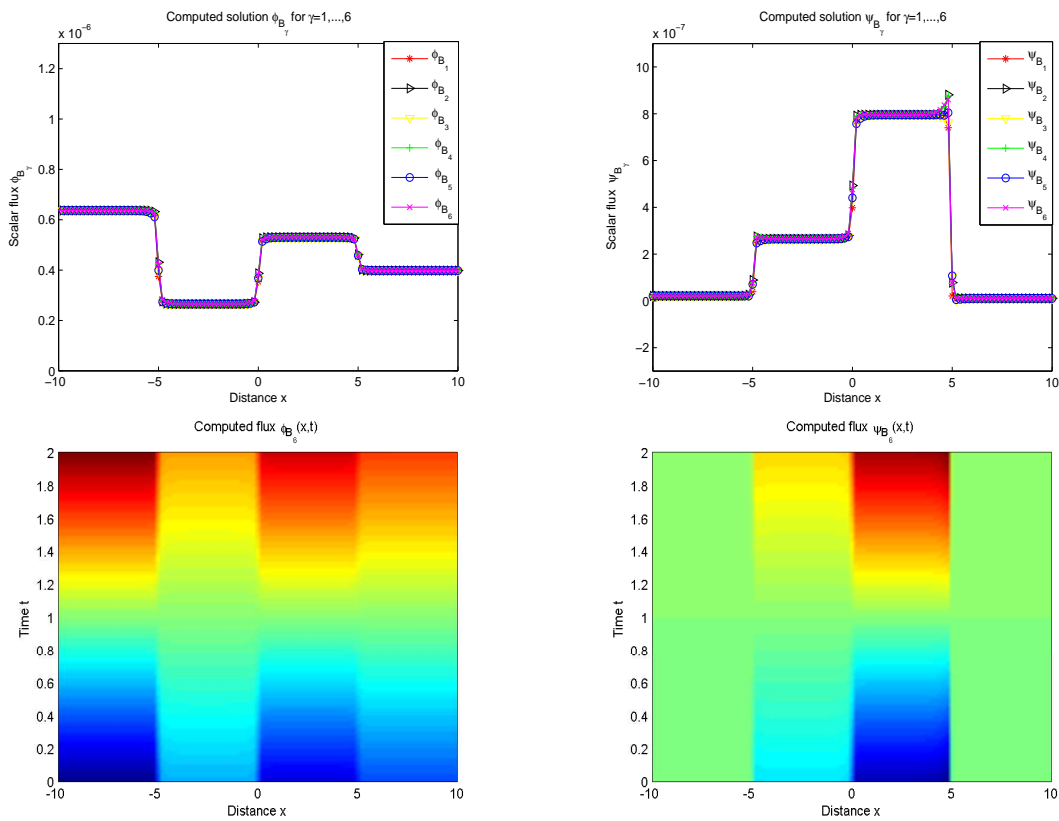


Figure 3: Cross sections at time $t = 2$ of the scalar flux ϕ_{B_γ} (left column) and Cross sections at time $t = 2$ of the scalar flux ψ_{B_γ} (right column).

In Figure 3 we present the snapshots of the scalar flux $\phi(x, t)$ at the bottom left and $\psi(x, t)$ at the bottom right using the (x, t) -meshgrid with 200×100 points. To visualize the effects of grids on the solution of the Fourier transform of this example, we illustrate in the top right, and top left the cross-sections of the scalar flux at the timeline $t = 2$. The obtained cross section results demonstrate the variability of solutions ϕ and ψ with respect to the magnetic permeability μ and the electrical permittivity ε piecewise functions. All results illustrated in Figure 3 are obtained with respect to the parameters $(\mu_1 = 5 * 10^6, \varepsilon_1 = 15 * 10^6)$, $(\mu_2 = 12 * 10^6, \varepsilon_2 = 1.2 * 10^6)$, $(\mu_3 = 6 * 10^6, \varepsilon_3 = 0.4 * 10^6)$ and $(\mu_4 = 8 * 10^6, \varepsilon_4 = 30 * 10^6)$. Figure 3 demonstrates the variation of the computed solutions ϕ and ψ concerning the different values of the magnetic permeability μ and the electrical permittivity ε . The computed results also justify the accuracy and robustness properties of the considered algorithm based on the Fourier Transform Discretization based on the quadrature formulae.

7.5. Convergence orders

In this example we solve the Maxwell’s problem (2.1)-(2.2)-(2.3) using constant magnetic permeability μ and constant electrical permittivity ε . The sources terms f and g , the boundary functions g_a, g_b, h_a and h_b and the initial datum ϕ_0 and ψ_0 are calculated such that the analytic solution of the problem (2.1)-(2.2)-(2.3) is given by $\phi_e(x, t) = \cos(x) \exp(-t^2)$ and $\psi_e(x, t) = \sin(x) \exp(-t^2)$, for all $(x, t) \in [-4, 4] \times [0, 1]$. All computations are used with the data $\mu = 10^6, \varepsilon = 10^5$.

The corresponding validation of convergence orders based on the theoretical results of Theorem 6.3 and Theorem 6.4 using all γ -splines function(for $\gamma = 1, \dots, 6$) given by $\|\Phi_e - \Phi_h\|_{L^2(\mathbb{R}; L^p \times L^p)} = \mathcal{O}(h^{\gamma+1})$ for $p = 1, 2, \infty$.

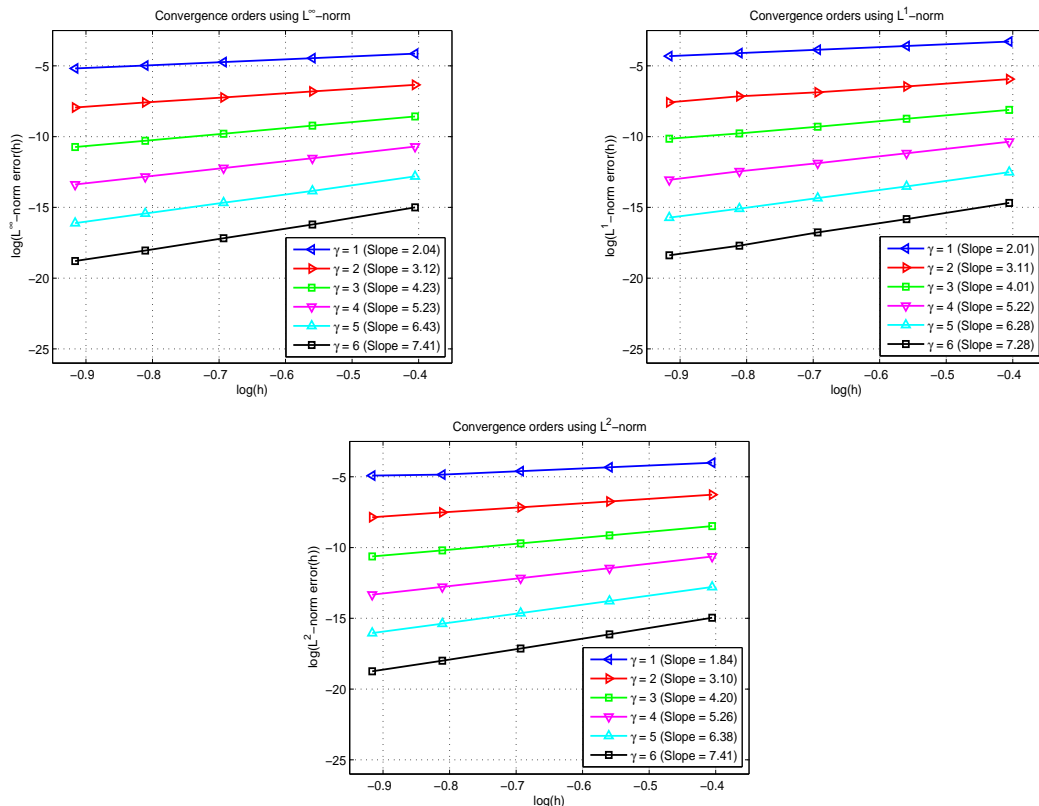


Figure 4: Illustration of the convergence orders using L^∞ -error norm, L^1 -error norm and L^2 -error norm, which agree theoretical error estimates presented in Theorem 6.5.

Let $E(h^{(k+1)})$ and $E(h^{(k)})$ be the errors obtained using the step sizes $h^{(k+1)}$ and $h^{(k)}$ respectively, so the practical Numerical Convergence Orders (NCO) are evaluated by using the following formula:

$$NCO := \log\left(\frac{E(h^{(k+1)})}{E(h^{(k)})}\right) / \log\left(\frac{h^{(k+1)}}{h^{(k)}}\right), \quad \text{where } h^{(k)} = \frac{b-a}{n^{(k)}}$$

where k is the iteration stage. Figure 4 illustrates the convergence orders of the approximation method based on γ -splines basis functions. We see that the numerical results agree with the theoretical error estimates presented in Section 6. It should be noted that in order to recover the outperform speed of convergence of the analytic solution ϕ_e , all standard quadrature methods (R.R. Method, L.R. Method, Trapezoidal Method, Simpson Method, and Gauss Method) are sufficient for evaluating the solution ϕ_e . Hence, the convergence orders $\gamma + 1$ is finally confirmed in the above figure for all error norm.

8. Conclusions

We have proposed the splines functions \mathbf{B}_γ of order γ and employed a Fourier transform approach to solve 1D version of Maxwell's equations. Firstly, we use the Fourier transform to change the time-dependent Maxwell equations into an equivalent problem depending on the frequency parameters. Using this technique, we avoid the redundancy of the time variable, which can occur throughout the discretization of the solution in the time domain. For each fixed frequency parameter, we have developed a Galerkin variational method based on the γ -splines interpolants as a solver of Maxwell's equations. Secondly, the time-domain solutions are obtained using the computations of the inverse Fourier transform based on the standard quadrature as Left-Rectangle Quadrature Method, Right-Rectangle Quadrature Method, Trapezoidal Quadrature Method, Simpson Quadrature Method, Gauss-Hermite Quadrature Method and Gauss Method. We also used the critical Nyquist frequency to evaluate the inverse Fourier transform when

the solutions depending on the time variable are not fast-decreasing functions. The Fourier transform method considered in this work removes the discretization of the time variable in Maxwell's equations. We provided some relevant numerical examples to illustrate our proposed method, and the results presented here prove the effectiveness of the Fourier transform approach and the splines finite method to solve the Maxwell equations. The performance and robustness of the higher order spline approximation is well validated by the Order of convergence.

References

1. M. Addam. *Approximation du Problème de Diffusion en Tomographie Optique et Problème Inverse*. Dissertation, LMPA, Université Lille-Nord de France, 2010.
2. M. Addam, A. Bouhamidi, and K. Jbilou. A numerical method for one-dimensional diffusion problem using Fourier transform and the B-spline Galerkin method. *Applied Mathematics and Computation*, 215: 4067–4079, 2010.
3. J. P. Berenger. A perfectly matched layer for the absorption of electromagnetic waves, *J. Comput. Physics*, 114(2): 185–200, 1994.
4. Brattka, V., and Yoshikawa, A., *Towards computability of elliptic boundary value problems in variational formulation*, *Journal of Complexity* 22 (2006) pp. 858-880.
5. Brézis, H., *Analyse Fonctionnelle: Théorie et applications*, Dunod, Paris, 1999.
6. A. Buffa, M. Costabel, and C. Schwab. Boundary element methods for Maxwell's equations on non-smooth domains. *Numerische Mathematik*, 92(4): 679-710, 2002.
7. A. Buffa, R. Hiptmair, T. Petersdorff, and C. Schwab. Boundary element methods for Maxwell transmission problems in Lipschitz domains. *Numerische Mathematik*, 95(3): 459–485, 2003.
8. C. Chu, P. Stoffa. Implicit finite-difference simulations of seismic wave propagation, *Geophysics*, 77(2): T57–T67, 2012.
9. C. de Boor. *A Practical Guide to Splines*. Springer-Verlag, New York, 1978.
10. G. C. Diwan, M. S. Mohamed, M. Seaïd, J. Trevelyan and O. Laghrouche, Mixed enrichment for the finite element method in heterogeneous media. *Int. J. Numer. Meth. Engng.* 101(1), 54-78 (2015).
11. M. Drolia, M. S. Mohamed, O. Laghrouche, M. Seaïd and J. Trevelyan, Enriched finite element method for initial-value problem of transverse electromagnetic waves in time domain. *Computer & Structures*. 101(1), 54-78 (2016).
12. Jin-Fa Lee, Robert Lee and Andreas Cangellaris. Time-Domain Finite-Element Methods. *IEEE Transactions on Antennas and Propagation*, Vol. 45, NO. 3, 430–442, 1997.
13. Y-Q. Li and H-C. Zhou. Experimental study on acoustic vector tomography of 2-D flow field in an experiment-scale furnace. *Flow Meas. Instrum.* 17: 113–122, 2006.
14. Ken Mattsson, Frank Ham and Gianluca Iaccarino. Stable and accurate wave-propagation in discontinuous media. *J. Comput. Physics*. 227: 8753–8767, 2008.
15. MATTHEW N. O. SADIKU *Numerical Techniques in ELECTROMAGNETICS with MATLAB*. CRC Press Taylor & Francis Group, Third Edition, New Jersey, 1973.
16. Frank Natterer. Reflection imaging without low frequencies. *Inverse Problems*. 27: 1–6, 2011.
17. M. H. Schultz and R. S. Varga. *L-splines*. *Numer. Math.* 10: 345–369, 1967.
18. M. H. Schultz. *Splines Analysis*. Prentice-Hall, Englewood cliffs, New Jersey, 1973.
19. H. Sielschott. Measurement of horizontal flow in a large scale furnace using acoustic vector tomography. *Flow Meas. Instrum.* 8: 191–197, 1997.
20. Lions, J. L., and Magenes, E., *Non-homogeneous Boundary Value Problems and Applications*, Vol. I, Springer, New York, 1972.
21. E. Perrey-Debain, J. Trevelyan, and P. Bettess. Plane wave interpolation in direct collocation boundary element method for radiation and wave scattering: numerical aspects and applications. *Journal of Sound and Vibration*, 261: 839–858, 2003.
22. E. Perrey-Debain, J. Trevelyan, and P. Bettess. Use of wave boundary elements for acoustic computations. *Journal of Computational Acoustics*, 11: 305–321, 2003.
23. E. Perrey-Debain, J. Trevelyan, and P. Bettess. Wave boundary elements: a theoretical overview presenting applications in scattering of short waves. *Engineering Analysis with Boundary Elements*, 28: 131–141, 2004.
24. H.C. Pocklington. Electrical oscillation in wire. *Cambridge Phil. Soc. Proc.*, Vol.9: 324–332, 1897.
25. A. Quarteroni and A. Valli. *Numerical approximation of partial differential equation*. Springer-Verlag, Berlin, 1994.
26. J. Sundnes, G. T. Lines, X. Cai, B. F. Nielson, K.-A. Mardal and A. Tveito. *Computing the Electrical Activity in the Heart*. Monographs in Computational Science and Engineering, Springer-Verlag, Berlin Heidelberg, 2010.

27. Sambit Das, Wenyuan Liao and Aniruch Gupta. An efficient fourth-order low dispersive finite difference scheme for a 2-D acoustic wave equation. *J. Comput. Appl. Math.* 270: 571–583, 2014.
28. Wenyuan Liao. On the dispersion, stability and accuracy of a compact higher-order finite difference scheme for 3D acoustic wave equation. *J. Comput. Appl. Math.* 258: 151–167, 2014.
29. Youneng Ma, Jinhua Yu and Yuanyuan Wang. An efficient complex-frequency shifted-perfectly matched layer for second-order acoustic wave equation. *Int. J. meth. Engng.* 97: 130–148, 2014.
30. K.S. Yee. Numerical solution of initial boundary value problems involving Maxwell’s equations in isotropic media. *IEEE Trans. Antenas Propag.* 14: 302–307, 1966.

Imad EL BARKANI,
MAO, LSA, ENSAH,
Abdelmalek Essaadi University,
BP 03, 32003 Ajdir, Al Hoceima, Morocco.
E-mail address: imad.elbarkani@etu.uae.ac.ma

and

Mohamed ADDAM (Corresponding Author),
MAO, LSA, ENSAH,
Abdelmalek Essaadi University,
BP 03, 32003 Ajdir, Al Hoceima, Morocco.
E-mail address: m.addam@uae.ac.ma